NATIONAL ADVISORY COMMITTEE FOR AERONAUTICS

TECHNICAL NOTE 1991

THEORETICAL LOADING AT SUPERSONIC SPEEDS OF FLAT SWEPT-BACK WINGS WITH INTERACTING TRAILING AND LEADING EDGES

By Doris Cohen

Ames Aeronautical Laboratory
Moffett Field, Calif.

Washington
December 1949

NATIONAL ADVISORY COMMITTEE FOR AERONAUTICS

TECHNICAL NOTE 1991

THEORETICAL LOADING AT SUPERSONIC SPEEDS OF FLAT SWEPT-BACK WINGS WITH INTERACTING TRAILING AND LEADING EDGES

By Doris Cohen

SUMMARY

By the method of superposition of conical flows, the load distribution is calculated for regions of a long, rectilinear, swept-back wing behind the points at which the Mach lines from the trailing-edge apex intersect the leading edge. It is found that a good approximation to the load can be obtained by the application of a fairly simple correction factor to the two-dimensional subsonic distribution. The similarity to two-dimensional flow is used to derive expressions for the loss of lift behind the Mach lines from the tips of the wing.

INTRODUCTION

In a previous paper (reference 1), formulas were derived by the superposition of linearized conical flows (reference 2) for the loading of a thin, flat, swept-back wing of rectilinear plan form traveling at supersonic speeds, under the limitation that the Mach lines from the trailing-edge apex did not cut the leading edge. Ahead of these Mach lines the flow is known to follow the conical pattern identified with the triangular wing having the same apex angle. By superposing an appropriate distribution of other conical flows behind the trailing edge to cancel the lift in the wake, the triangular-wing loading can be corrected within the region behind the trailing-edge Mach lines to conform to the Kutta condition for a subsonic trailing edge. This method is described more fully in reference 1.

When the region of influence of the trailing edge includes a part of the leading edge and the stream ahead of it, the mutual interaction of the two regions results in a flow which is susceptible to treatment by the conical-flows method only at the expenditure of considerable effort. The flow in the tip regions is particularly difficult to calculate. A method of cancellation of external lift by supersonic doublet distributions, proposed in reference 3, offers some promise of providing a solution in the tip region if the pressure at all points inboard of the tip Mach cone is known from other sources. The method appears, however, to be in error as applied in the neighborhood of the leading edge or of a raked-out tip. Formulas of considerable simplicity have been derived by Heaslet, Lomax,

and Spreiter (reference 4), but only for a particular family of slightly tapered wings with a filleted trailing edge and plan forms very slender relative to the Mach cone.

Since no satisfactory method appeared to be available for investigating the general problem of the rectilinear swept-back wing with interacting leading and trailing edges – that is, wings of high sweep or aspect ratio, or wings of moderate sweep and aspect ratio at low supersonic Mach numbers – the work of reference 1 was extended, with some simplifying assumptions for the tip regions, to cover such cases. The principal object of the investigation was to obtain, if possible, an indication of the manner in which the flow in the outboard regions of a long narrow wing approaches the subsonic two-dimensional type of flow indicated by simple sweep theory.

The calculations showed that the section loading assumes the general shape of the subsonic two-dimensional loading at the very station at which the trailing-edge Mach line intersects the leading edge. Further investigation showed that everywhere behind the Mach lines from the point of intersection and farther outboard the load could be closely approximated by a fairly simple adaptation of the two-dimensional formulas.

The following material outlines the method of obtaining the load distribution in the region of leading- and trailing-edge interaction by the superposition of conical flows and presents the formulas for approximating the results by a single step based on correction of the two-dimensional formulas. A corresponding approximate correction to the load near the tips is also derived.

CALCULATION OF LOADING BY SUPERPOSITION OF CONICAL FLOWS

Procedure

Figure 1 shows the central portion of a long, narrow, swept-back wing divided into various regions by the trailing-edge Mach lines, the Mach line arising at the intersection of the trailing-edge Mach line with the leading edge, and so on. In the superposition process to be described, these Mach lines mark the regions of influence of the flow fields used in successive cancellations of lifting pressure outside the wing boundaries.

In region I, the streamwise component u of the upper-surface perturbation velocity – to which, in linear theory, the loading is proportional – is given, as previously mentioned, by the known solution for the triangular wing swept behind the Mach cone

$$u_{\Delta}(a) = \frac{m\, u_o}{\sqrt{m^2 - a^2}} \qquad (1)$$

where u_o, the constant velocity along the center line a=0, is

$$u_o = \frac{mV\alpha}{\beta\, E(\sqrt{1-m^2})} \tag{2}$$

(See Appendix A for explanation of the symbols.)

The flow over the remainder of the wing, however, is affected by the reduction of the lift to zero behind the trailing edge. The primary induction effects on the wing are given in reference 1 in the form of two corrections to the basic perturbation velocity: a symmetrical correction[1]

$$(\Delta u)_o = -u_o \frac{F(\sqrt{1-m_t^2}, \varphi)}{K(\sqrt{1-m_t^2})} \tag{3}$$

with

$$\varphi = \sin^{-1}\sqrt{\frac{1-t_o^2}{1-m_t^2}}$$

and the integral with respect to a of

$$(\Delta u)_a = -\frac{u_a}{\pi}\cos^{-1}\frac{(1-a)(t_a-m_t) - (m_t-a)(1-t_a)}{(1-m_t)(t_a-a)} \tag{4}$$

where $u_a = (du_\Delta/da)da$.

These induced velocities appear on the wing surface (in regions II, III, . . .) as corrections to the basic velocity u_Δ. Beyond the actual surface of the wing they represent a discontinuity in pressure which cannot be supported in the free stream and must therefore be canceled at all points ahead of the leading edge. Cancellation of these pressure differences will, in turn, induce additional corrections to the perturbation velocities in region III and all portions of the wing aft of that region. Again, pressure differences will be introduced in the wake region and new corrections will have to be made which will affect the loading in region IV and all more rearward portions of the wing. For the present no tip location will be specified, except that it is, of course, outboard of the intersection of the first trailing-edge Mach line with the leading edge. The tip region will be considered after the result of the trailing-edge – leading-edge interference effect is determined.

[1]Equation (3) as originally prescribed in reference 1 (equation (51)) is incorrect. An errata sheet has been issued to correct this error.

The initial distribution of lift to be canceled ahead of the wing (in region II extended) is the result of superposing an infinite number of conical flow fields originating at the various points on the trailing edge. To cancel this distribution of lift by the superposition of conical flows requires that each of the lift distributions corresponding to a single value of a in equation (4), as well as the lift due to $(\Delta u)_o$ (equation (3)), be canceled separately by an infinite number of conical fields.

The single conical field of $(\Delta u)_o$ will be considered first. The velocity field to be superimposed ahead of the leading edge to cancel the velocities $(\Delta u)_o$ induced in the plane of the wing by the symmetrical solution (equation (3)) can be built up, as shown in the sketch on the left,

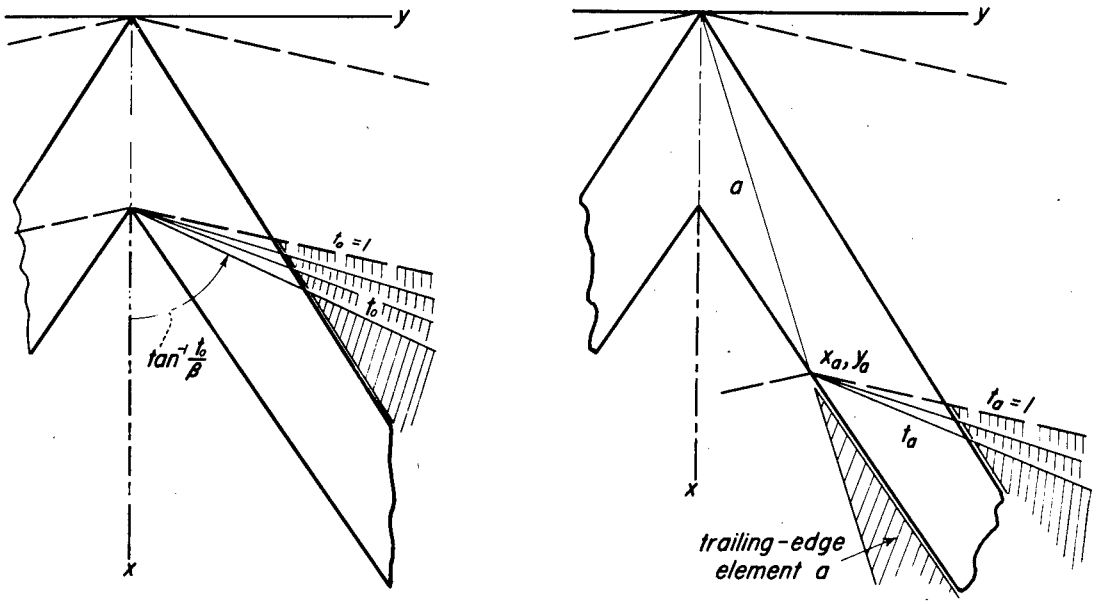

of overlapping constant-velocity sectors having one edge along the leading edge of the wing and one along the extended ray t_o from the apex of the trailing edge. The magnitude of the constant velocity on each element is $[d(\Delta u)_o/dt_o]\, dt_o$ or, from equation (3),

$$\frac{u_o\, dt_o}{K(\sqrt{1-m_t^2})\sqrt{(1-t_o^2)(t_o^2-m_t^2)}} \tag{5}$$

Similarly, for each oblique wake or trailing-edge element a, (see right-hand sketch), a canceling field can be built up ahead of the leading edge by the superposition of sectors bounded by the leading edge and by rays t_a from the apex x_a, y_a of the element a and having a constant velocity of magnitude

$$\frac{\partial(\Delta u)_a}{\partial t_a} dt_a = -\frac{1}{\pi} u_a \frac{\partial}{\partial t_a} \cos^{-1} \frac{(1-a)(t_a-m_t)-(m_t-a)(1-t_a)}{(1-m_t)(t_a-a)} dt_a$$

(from equation (4)).

Elementary Solution for the Region Ahead of the Leading Edge

In general, the elementary solution required for the cancellation of pressure in the plane of the wing ahead of the leading edge is one that:

1. Provides constant streamwise velocity over an infinite sector bounded on one side by the leading edge of the wing (extended) and on the other by an arbitrary ray extending outward into the stream from some point x_b,y_b on the leading edge. (See fig. 2.)

2. Induces no vertical velocity, or downwash, on the wing.

3. Induces no lift except on the wing and within the sector described in condition (1).

At first glance these conditions would appear to be satisfied by the oblique solutions used at the trailing edge in the previous work, if properly oriented with respect to the wing, and one might expect the same form of solution to apply. In reference 1, however, it was pointed out that the downwash connected with this solution remained constant over the wing, only provided that the wing area did not include the line y = constant extending downstream from the apex of the element. In the case of the leading-edge element this condition is violated (fig. 2) and an additional term is needed to bring the downwash to zero throughout the area of the wing affected by the element.

The solution applicable to this case has been given by Lagerstrom (reference 2). The u component of the velocity in the plane of the wing is as follows:

$$u = \text{r.p.} \frac{u_b}{\pi} \left[\cos^{-1} \frac{(t_a-m)(1+t_b)-(m-t_b)(1+t_a)}{(1+m)(t_b-t_a)} - \frac{2m}{(1+m)t_a} \sqrt{(t_a-m)(1+t_a)} \sqrt{\frac{1+t_b}{m-t_b}} \right] \tag{6}$$

In equation (6), u_b is the constant streamwise perturbation velocity over the element, and t_b is β times the inclination, with respect to the stream, of the ray from the apex x_b,y_b of the element

through the point x,y at which the pressure is being computed. Thus,

$$t_b = \frac{\beta(y-y_b)}{x-x_b} \tag{7}$$

When the correction is being made for the symmetrical trailing-edge element only, t_a is replaced by t_o and $u_b = [d(\Delta u)_o/dt_o]\, dt_o$.

For brevity, the two parts of the correction function will be referred to as

$$C(t_a) = \text{r.p.}\ \cos^{-1} \frac{(t_a-m)(1+t_b)-(m-t_b)(1+t_a)}{(1+m)(t_b-t_a)} \tag{8}$$

and

$$R(t_a) = \text{r.p.}\ \frac{-2m}{(1+m)t_a} \sqrt{(t_a-m)(1+t_a)}\sqrt{\frac{1+t_b}{m-t_b}} \tag{9}$$

These functions and the induced velocity (equation (6)) are plotted against t_b in figure 2 for typical values of the other parameters.

Leading-Edge Corrections to the Local Lift

Applying equation (6) to the cancellation of the symmetrical-wake-correction velocities $(\Delta u)_o$ ahead of the wing results in the following induced-velocity increment at any point x,y on the wing:

$$(\Delta u_b)_o = \frac{1}{\pi} \int_{\tau_o}^{1} \frac{d(\Delta u)_o}{dt_o} [C(t_o) + R(t_o)]\, dt_o \tag{10}$$

where τ_o is that value of t_o for which $t_b = -1$, and designates the most rearward leading-edge element containing the point x,y within its Mach cone. In terms of x and y,

$$\tau_o = \frac{m(x+\beta y)}{(x+\beta y)-(1+m)c_o} \tag{11}$$

Integration of $\frac{d(\Delta u)_o}{dt_o} C(t_o)dt_o$ is not possible by elementary means. For values of m equal to or greater than 0.4, a series expansion can be used for $(\Delta u)_o$ (Appendix B) and a satisfactory expression found for the

first term of the integral (equation (10)). Calculations for $m = 0.2$ indicate that integration by series may not be sufficiently accurate when m is small. In such a case, the first part of the integration may be performed graphically.

The second part of equation (10) can be integrated in closed form as follows:

$$\frac{1}{\pi}\int_{\tau_o}^{1} \frac{d(\Delta u)_o}{dt_o} R(t_o)\, dt_o = \frac{-4m^{3/2}u_o}{\pi m_t(1+m)K'(m_t)}\sqrt{\frac{x+\beta y}{mx-\beta y}}\left[KE(k,\psi)-EF(k,\psi)\right] \qquad (12)$$

where K and E are the complete elliptic integrals of the first and second kind, respectively, of the modulus

$$k = \sqrt{\frac{2m_t(1-\tau_o)}{(1-m_t)(\tau_o+m_t)}} \qquad (13)$$

and $F(k,\psi)$ and $E(k,\psi)$ are the corresponding incomplete integrals, with the argument

$$\psi = \sin^{-1}\sqrt{\frac{\tau_o+m_t}{2\tau_o}} \qquad (14)$$

The corresponding procedure for each oblique trailing-edge element a results in an expression for $[d(\Delta u)_b/da]\, da$ similar to equation (10). Again, the first term cannot be integrated in closed form; the second term becomes

$$\frac{1}{\pi}\int_{\tau_a}^{1}\frac{\partial(\Delta u)_a}{\partial t_a} R(t_a)\, dt_a = \frac{-4m\, u_a\sqrt{1-a}}{\pi^2(1+m)a}\sqrt{\frac{(m_t-a)(x+\beta y)-(1+m)m_t c_o}{mx-\beta y}} \times$$

$$\left\{\sqrt{\frac{(1+a)(\tau_a-a)}{(1-a)(m_t-a)}}\left[KE(k_a,\psi_a)-EF(k_a,\psi_a)\right]-\right.$$

$$\left.\sqrt{\frac{\tau_a}{m_t}}\left[KE(k_a,\psi_o)-EF(k_a,\psi_o)\right]\right\} \qquad (15)$$

where

$$\tau_a = \frac{m(m_t-a)(x+\beta y)-am_t c_o(1+m)}{(m_t-a)(x+\beta y)-m_t c_o(1+m)} \qquad (16)$$

$$k_a = \sqrt{\frac{(1+m_t)(1-\tau_a)}{(1-m_t)(1+\tau_a)}} \tag{17}$$

$$\psi_a = \sin^{-1}\sqrt{\frac{(m_t-a)(1+\tau_a)}{(\tau_a-a)(1+m_t)}} \tag{18}$$

$$\psi_o = \sin^{-1}\sqrt{\frac{m_t(1+\tau_a)}{\tau_a(1+m_t)}} \tag{19}$$

In region III (fig. 1), the total leading-edge correction to the perturbation velocity at any point x,y is

$$(\Delta u)_b = (\Delta u_b)_o + \int_o^{a_o'} \frac{d(\Delta u)_b}{da}\, da \tag{20}$$

where a_o' corresponds to the most rearward trailing-edge element the velocity field of which, reflected in the leading edge, can affect the point x,y.

In region IV, the cancellation of the velocity increment $(\Delta u)_b$ at the trailing edge must be taken into account. To do this in any rigorous way is obviously impractical. However, the velocities to be canceled are small, and it is possible to estimate the effect of their cancellation in many cases. Beyond region IV the velocity distribution cannot be determined in practice, except very approximately, by the conical-flows method.

Calculated Results

Load distributions have been calculated by the foregoing method for three combinations of taper, sweep, and Mach number as follows:

	Untapered		Tapered
m =	0.2	0.4	0.4
m_t =	0.2	0.4	0.6

These values of m and m_t represent, by virtue of the Prandtl-Glauert transformation, a variety of practical sweep angles at Mach numbers between 1 and 2; as for example, 0.2 would be the value of m for a wing with 63° sweep of the leading edge at a Mach number of 1.075, or 75° sweep

at a Mach number of 1.25. Similarly, $m = 0.4$ would correspond to 45° of sweep at $M = 1.08$, 60° at $M = 1.22$, or 75° at $M = 1.80$. The trailing-edge sweep angles at these latter Mach numbers, if $m_t = 0.6$, are $34^\circ 13'$, 49°, and 68°, respectively.

In figure 3, the $m = 0.4$ wings are shown at $M = \sqrt{2}$, so that $\Lambda = \cot^{-1} 0.4$. Keeping the same angle of sweep, the $m = 0.2$ case is depicted (fig. 4) as representing the same wing at a lower Mach number ($\beta = 1/2$). Figures 3 and 4 show also the spanwise stations at which the load distributions were calculated.

The results of the calculations are presented (figs. 5, 6, and 7) in the form of values of $\beta\,(\Delta p/q\alpha)$ where Δp is the local lift, q the free-stream dynamic pressure, and α the angle of attack. In linear theory this quantity is connected with the streamwise component of the upper-surface perturbation velocity u by the relation

$$\frac{\Delta p}{q\alpha} = 4\,\frac{u}{V\alpha}$$

The various components of the lift, as calculated by the superposition method, are shown individually.

Figure 5 presents the resulting lift distributions at the two stations of the tapered wing shown in figure 3. Section A-A contains the intersection of the trailing-edge Mach line with the leading edge, so that the leading-edge correction at the leading edge is zero. At points farther back along the leading edge, as at $\beta y/c_o = 0.8$, the correction is minus infinity. However, it is seen to increase to a small positive value within a fraction of the chord length at $\beta y/c_o = 0.8$.

At both stations it is necessary to estimate the effect of cancellation of the leading-edge correction at the trailing edge to satisfy the Kutta condition. Cancellation would be effected by means of oblique elements of the type used previously (equation (4)) in canceling lift at the trailing edge, so that the induced lift on the wing has the same general shape as the primary oblique trailing-edge correction. It therefore may be presumed to fall along a modified inverse-cosine curve to zero at the boundary of the region affected. Locating this boundary, the twice-reflected Mach line from the trailing-edge apex, we are able to draw in a satisfactory estimate (dotted curve) of the correction to bring the pressure once more to zero at the trailing edge.

The untapered wing with the same sweep ($m = 0.4$) relative to the Mach lines is shown in figure 6 with the load distributions calculated at the same stations.

Four section lift distributions are presented (fig. 7) for $m = 0.2$. At $\beta y/c_o = 0.15$ only the rear 60 percent is influenced by the subsonic

trailing edge. The reflection of this influence in the leading edge alters the pressure over the rear 40 percent of the section. At section B–B the leading- and trailing-edge interaction affects the entire section. A further reflection of this effect in the trailing edge must be estimated.

At section C–C the reflection of the leading-edge correction in the trailing edge covers the whole extent of the chord and any estimate of its magnitude would be necessarily arbitrary. Also, a second pair of reflections must be taken into account. The final pressure distribution has therefore been drawn as a band within which the true curve may be shown to lie. Its height is the error introduced at the trailing edge by the first leading-edge correction, except very near the leading edge, where an infinite negative correction is known to be introduced by the second leading-edge correction. The calculations were also carried out for $\beta y/c_o = 0.45$. The margin of uncertainty was found not to have increased by any appreciable amount. (See fig. 7(d).)

It may be seen from the figures that, except in the vicinity of the leading edge, the magnitude of the leading-edge correction is small. The part due to reflecting the oblique trailing-edge correction is roughly the same fraction of the total leading-edge correction as the oblique trailing-edge correction is, at the leading edge, of the total trailing-edge correction. This fraction is less than 10 percent in the examples calculated and the resulting contribution to the leading-edge correction is negligible. The labor involved in computing the loading can in such cases be considerably reduced by omitting the calculation of the effect of reflecting the oblique trailing-edge correction in the leading edge.

APPLICATION OF TWO-DIMENSIONAL FORMULAS TO CALCULATION OF LOAD DISTRIBUTION

Load on Midspan Portion of Wing

It is apparent from the calculated results that, whenever the plan form and the Mach number are such that the trailing-edge Mach line intersects the leading edge, the load distribution behind the Mach lines from the point of intersection (regions III and beyond, fig. 1) resembles in shape the well-known incompressible load distribution over an infinitely long flat plate. However, the quantitative agreement does not appear good, particularly in the case of the tapered wing, until the load distributions over sections normal to the stream are examined, when a simple proportionality of the curves is observed. In order to determine the factor of proportionality it is noted that, if the curves are similar, each can be characterized by the strength of the singularity at the leading edge. An explicit expression for this quantity can be obtained

for regions III and IV[2] of the swept-back wing, and the ratio of this quantity to the corresponding quantity in the two-dimensional flow is the required correction factor to bring the two curves into agreement.

The leading-edge singularity in the loading on the swept-back wing is initially that in the triangular-wing loading. Introduction of the leading-edge corrections to the load in region III reduces the strength of the singularity there through the terms $R(t_o)$ and $R(t_a)$. (The inverse-cosine function is always finite.)

It is convenient to define the strength of the leading-edge singularity as the coefficient of $(mx-\beta y)^{1/2}$ in the velocity distribution. In the region ahead of the trailing-edge Mach line, this coefficient is, from equation (1),

$$\frac{mxu_o}{\sqrt{mx+\beta y}}$$

reducing to

$$C_\Delta = u_o \sqrt{\frac{mx}{2}} \tag{21}$$

at the leading edge.

From equations (12) and (15), decrements to this coefficient may be derived for the portion of the leading edge behind the intersection with the trailing-edge Mach line, as follows:

$$(\Delta C)_o = \frac{-4mu_o}{\pi m_t K'(m_t)} \sqrt{\frac{mx}{1+m}} \left[KE(k,\psi) - EF(k,\psi) \right] \tag{22}$$

and, for each value of a from 0 to that value a_o which makes τ_a equal to one,

$$\frac{d\Delta C}{da} da = \frac{-4m}{\pi^2\sqrt{1+m}} \frac{u_a}{a} \sqrt{1-a} \sqrt{(m_t-a)x-m_t c_o} \left\{ \sqrt{\frac{(1+a)(\tau_a-a)}{(1-a)(m_t-a)}} \left[KE(k_a,\psi_a) - \right.\right.$$

$$\left.\left. EF(k_a,\psi_a) \right] - \sqrt{\frac{\tau_a}{m_t}} \left[KE(k_a,\psi_o) - EF(k_a,\psi_o) \right] \right\} \tag{23}$$

[2]This expression will be shown later to hold approximately for some distance outboard of its theoretical limit of applicability, that is, beyond region IV (fig. 1).

where τ_o and τ_a reduce to

$$\tau_o = \frac{mx}{x-c_o}$$

and

$$\tau_a = \frac{(m_t-a)mx-m_t c_o a}{(m_t-a)x-m_t c_o}$$

and the arguments and moduli of the elliptic integrals follow as for equations (12) and (15).

The coefficient of $(mx-\beta y)^{-1/2}$ in region III is therefore

$$C_\Delta + (\Delta C)_o + \int_o^{a_o} \frac{d\Delta C}{da}\, da$$

with

$$a_o = m_t \frac{c_o-(1-m)x}{m_t c_o-(1-m)x} \tag{24}$$

For convenience, we may define the nondimensional coefficient

$$\sigma(x) = \frac{1}{V\alpha\sqrt{c_o}} \left[C_\Delta + (\Delta C)_o + \int_o^{a_o} \frac{d\Delta C}{da}\, da \right] \tag{25}$$

In figure 8, the quantity $\beta\sigma(x)$ is plotted against x/c_o for the wings previously discussed. Additional terms enter into the coefficient at the values of x/c_o indicated by cross-markings on the curves, where successive reflections of the Mach lines off the trailing edge intersect the leading edge. Evaluation of these terms has not been attempted; however, the asymptotes of the curves for the untapered wings are known from simple sweep theory, and it is apparent from the figure that the magnitude of the omitted decrements, within the practical range of aspect ratios, must be small. The curve for the tapered wing, without the additional corrections, goes to zero where the wing tapers to a point, at $x = 3c_o$. However, the complete curve, with the effect of the successive reflections included, would have a finite value at that point. It can be shown that the successive corrections enter with zero derivatives of successively higher order so that the error caused by neglecting one is initially small. The curve in figure 8 is believed valid to the extent of the solid line.

The subsonic perturbation velocity on an infinitely long flat plate moving normal to its surface with circulation Γ is

$$\frac{\Gamma}{\pi c}\sqrt{\frac{1-\eta}{\eta}} \tag{26}$$

where η is the distance to the leading edge, expressed as a fraction of the chord c. If the section of the plate coincides with a section of the swept-back wing taken perpendicular to the stream (x constant), as in the sketch, then the chord length is

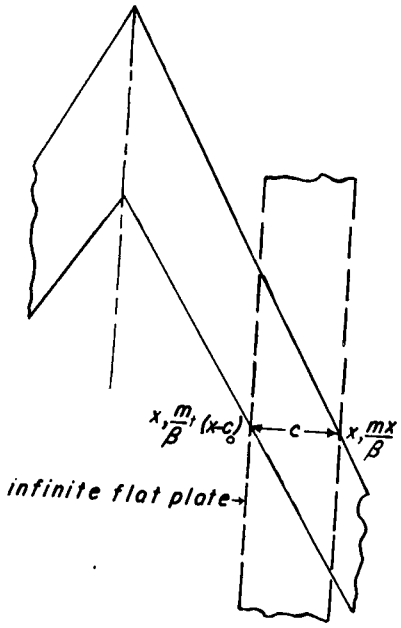

$$\frac{1}{\beta}\left[mx-m_t\,(x-c_o)\right] \tag{27}$$

and

$$\eta = \frac{mx-\beta y}{mx-m_t(x-c_o)} \tag{28}$$

Substituting for η in equation (26), we find that the coefficient of $(mx-\beta y)^{-1/2}$ is

$$\frac{\Gamma}{\pi c}\sqrt{\beta y-m_t(x-c_o)} \tag{29}$$

which reduces at the leading edge to

$$\frac{\Gamma}{\pi c}\sqrt{mx-m_t(x-c_o)}$$

Equating this coefficient to the coefficient for the swept-back wing gives

$$\frac{\Gamma}{\pi c} = \frac{1}{\sqrt{mx-m_t(x-c_o)}}\left[C_\Delta + (\Delta C)_o + \int_o^{a_o}\frac{d\Delta C}{da}\,da\right] \tag{30}$$

Then the two-dimensional approximation to the load coefficient on the outboard portions of a swept-back wing is given by

$$\frac{u}{V\alpha} = \sigma(x)\sqrt{\frac{[\beta y - m_t(x-c_o)]c_o}{[mx - m_t(x-c_o)](mx-\beta y)}} \tag{31}$$

or

$$\frac{\Delta p}{q\alpha} = 4\sigma(x)\sqrt{\frac{[\beta y - m_t(x-c_o)]c_o}{[mx - m_t(x-c_o)](mx-\beta y)}} \tag{32}$$

The closeness with which the foregoing procedure predicts the theoretical loading over swept-back wings is indicated by figures 9, 10, and 11, where the previously calculated load distributions are compared with those calculated by equation (32). Even in the case of the highly tapered wing, the agreement is seen to be good.

At the most inboard section of the $m = 0.2$ wing (fig. 7(a)) there is, of course, no agreement over the forward portion where the flow is essentially conical, but behind the reflection of the trailing-edge Mach line in the leading edge (at 60-percent chord) the adjusted two-dimensional theory appears to hold fairly well. At the next section, B-B, the agreement is very good. At sections C-C and D-D, the curve calculated by the two-dimensional theory lies within the band prescribed for the loading by the conical-flow calculations. Since the discrepancy between the two-dimensional loading and the correct theoretical distribution is already, at section B-B, less than the width of the bands in figures 7(c) and (d), and must diminish to zero at infinity, it may be supposed that the corrected two-dimensional curve is at least as satisfactory an approximation to the correct curves at sections C-C and D-D as at section B-B, and more satisfactory than can be obtained by the conical-flows method.

The load distributions derived by simple sweep theory are included (figs. 9(b), 10(b), and 11(d)) to show the magnitude of the plan-form effect and also, in the case of the untapered wings, the curves which the load distributions are approaching with increasing distance from the plane of symmetry.

In figures 10(b) and 11(b), comparison is also made with results of the slender-wing theory of reference 4. In the second case (fig. 11(b)), the Mach line from the trailing edge of the root chord, in the modified plan form of reference 4, crosses the section at 12.6 percent of the chord, causing the cusp which appears in the load distribution calculated for that wing. It is interesting to note that the loadings calculated by the two methods agree fairly well even when the wing violates the slender plan-form assumption ($m=0.4$).

Calculation of Tip Effect

In the conical-flows method, the effect on the load distribution of the presence of the wing tip is calculated by canceling, outboard of the tip, each of the various components of the lifting pressure previously calculated. To do this exactly when the trailing-edge Mach line and leading edge intersect involves a prohibitive amount of work. Approximate procedures have been developed (Appendix C), but the calculations remain tedious, while the accuracy is in some respects unsatisfactory. A simpler approximation, based on the assumption of cylindrical flow beyond the tip location, was therefore attempted. The formulas are developed for the tips alined with the stream, but the fundamental procedure may be applied to raked tips as well.

It is assumed that the velocity distribution to be canceled in the plane of the wing outboard of the tip is an extension of the velocity distribution calculated for the tip section along lines parallel to the leading edge. For this purpose the approximate load distribution given by equation (32) is used, still further simplified by assuming σ to remain constant at its value at the leading edge of the tip section. The error involved in this assumption may be estimated by referring to figure 8. The maximum range of abscissa to be used is 1.0; the change in ordinate within that range — where the influence of the wake is effective — is less than 10 percent. (Where the wing is tapering to a point and σ is changing more rapidly, the tip region is so small that the entire calculation of tip effects would probably be omitted.)

The assumption of constant σ results in a failure to cancel exactly the lift along the tip. The assumption of cylindrical flow, while reasonable for the untapered wing (compare figs. 10(a) and (b), for example) would appear to be too drastic for the tapered wing, where neither the chord nor the loading remains constant. However, it has been shown in reference 1 that the major part of the tip effect results from the cancellation of the infinite pressure along the leading edge, and this part will be accurately calculated. The effect of the residual lift on the rearward portion of the tip section and in the stream will be shown, by numerical examples, to be small.

The distribution of perturbation velocity at the tip station $y = s$ with the simplification of constant σ is, from equation (31), approximately

$$u(x_c,s) = \sigma_s V\alpha \sqrt{\frac{[\beta s - m_t(x_c - c_o)]\ c_o}{[mx_c - m_t(x_c - x_o)\,](mx_c - \beta s)}} \qquad (33)$$

where x_c,s are the coordinates of a point on the tip and σ_s is the value of σ at $x = \beta s/m$.

This expression may be more conveniently written in terms of the variable

$$\xi_c = \frac{x_c-(\beta s/m)}{c_t} \qquad (34)$$

which is the ratio of the distance of x_c,s back of the leading edge (see sketch) to the tip chord c_t. Since

$$c_t = \left(c_o + \frac{\beta s}{m_t}\right) - \frac{\beta s}{m} \qquad (35)$$

equation (33) may be written

$$u(x_c,s) = \frac{\sigma_s V\alpha}{\sqrt{mc_t}} \sqrt{\frac{(1-\xi_c)c_o}{\left(1-\frac{m_t-m}{m_t}\xi_c\right)\xi_c}} \qquad (36)$$

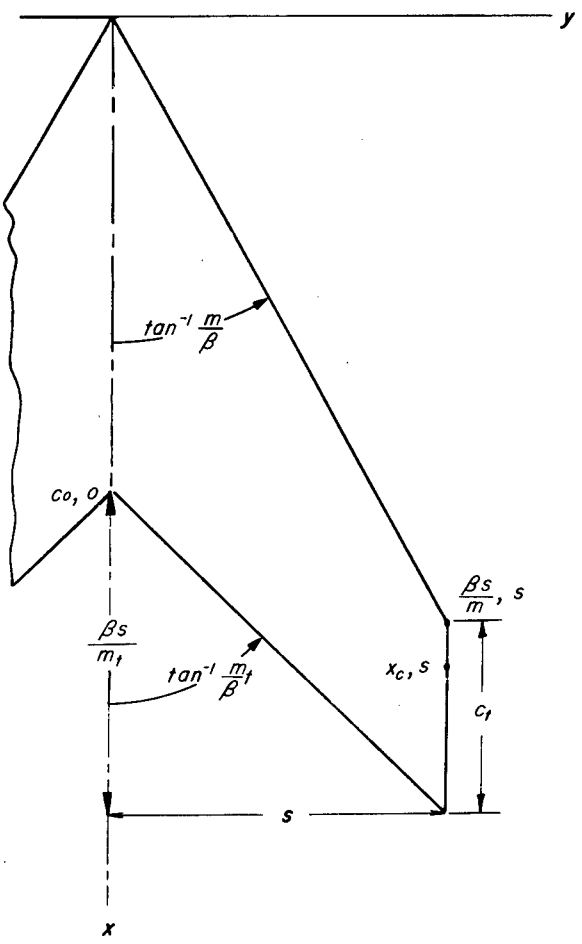

If the velocity distribution u is assumed to be constant beyond $y = s$ along lines parallel to the leading edge, it may be canceled by the superposition of conical constant-velocity elements, having one edge along the tip and the other parallel to the leading edge, with apexes displaced along the tip by increments in ξ_c. The velocity induced at a point x,y by each such element would be (reference 2)

$$\frac{u_c}{\pi} \cos^{-1} \frac{m+t_c+2mt_c}{t_c-m} \qquad (37)$$

where

$$t_c = \frac{\beta(y-s)}{x-x_c} \qquad (38)$$

and u_c is the velocity on each sector.

Following the procedure used in deriving equation (36) in reference 1, the corresponding equation may be written for the velocities induced by

canceling the assumed cylindrical loading:

$$\frac{\Delta u}{V\alpha} = \frac{-\sqrt{m(1+m)(x-x_o)}}{\pi} \int_{\frac{\beta s}{m}}^{x_o} \frac{u(x_c,s)}{V\alpha} \frac{dx_c}{[(1+m)x-x_o-mx_c]\sqrt{x_o-x_c}} \tag{39}$$

where x_o,s is the intersection of the Mach forecone from x,y with the tip.

If the distances of x,y and x_o,s back of the leading edge, measured as fractions of the tip chord, are

$$\xi = \frac{1}{c_t}\left(x - \frac{\beta y}{m}\right) \tag{40}$$

and

$$\xi_o = \frac{1}{c_t}\left(x_o - \frac{\beta s}{m}\right) \tag{41}$$

it can be shown that

$$(1+m)(x-x_o) = mc_t(\xi-\xi_o) \tag{42}$$

from which equation (39) can be written (with the substitution for $u(x_c,s)$ from equation (36))

$$\frac{\Delta u}{V\alpha}(x,y) = -\frac{\sigma_s\sqrt{\xi-\xi_o}}{\pi\sqrt{m\lambda}} \int_o^{\xi_o} \frac{d\xi_c}{\xi-\xi_c\sqrt{(\xi_o-\xi_c)\left(1-\frac{m_t-m}{m_t}\xi_c\right)\xi_c}} \tag{43}$$

where $\lambda = \frac{c_t}{c_o}$, the taper ratio.

In integrating equation (43), three cases must be distinguished: (1) $\xi < 1$ (always true for the untapered wing), (2) $1 < \xi < \frac{m_t}{m_t-m}$ (when the point x,y lies behind the trailing edge of the fictitious untapered wing through the tip chord), and (3) $\xi > \frac{m_t}{m_t-m}$ (a possible condition for some points near the trailing edge of a highly swept or tapered wing).

In the first case $(\xi < 1)$

$$\frac{\Delta u}{V\alpha}(x,y) = \frac{-2\sigma_s}{\pi\sqrt{m\lambda}} \left\{ \frac{m}{m_t\left(1-\frac{m_t-m}{m_t}\,\xi\right)} \sqrt{\frac{\xi-\xi_o}{1-\frac{m_t-m}{m_t}\,\xi_o}}\; K + \right.$$

$$\left. \sqrt{\frac{1-\xi}{\xi\left(1-\frac{m_t-m}{m_t}\,\xi\right)}} \left[KE(k',\psi_1) - (K-E)F(k',\psi_1)\right] \right\} \quad (44a)$$

where K and E are the complete elliptic integrals of modulus

$$k = \sqrt{\frac{m\xi_o}{m_t\left(1-\frac{m_t-m}{m_t}\,\xi_o\right)}}$$

and $E(k',\psi_1)$ and $F(k',\psi_1)$ are the incomplete integrals, with the complementary modulus

$$k' = \sqrt{\frac{1-\xi_o}{1-\frac{m_t-m}{m_t}\,\xi_o}}$$

and argument

$$\psi_1 = \sin^{-1}\sqrt{\frac{(1-\xi)\left(1-\frac{m_t-m}{m_t}\,\xi_o\right)}{(1-\xi_o)\left(1-\frac{m_t-m}{m_t}\,\xi\right)}}$$

In the second case $\left(1 < \xi < \frac{m_t}{m_t - m}\right)$

$$\frac{\Delta u}{V\alpha}(x,y) = \frac{-2\sigma_s}{\pi\sqrt{m\lambda}} \left\{ \frac{1}{\xi} \sqrt{\frac{\xi - \xi_o}{1 - \frac{m_t - m}{m_t}\xi_o}}\, K - \right.$$

$$\left. \sqrt{\frac{\xi - 1}{\xi\left(1 - \frac{m_t - m}{m_t}\xi\right)}}\, [KE(k,\psi_2) - EF(k,\psi_2)] \right\} \quad (44b)$$

where

$$\psi_2 = \sin^{-1} \sqrt{\frac{m_t\left(1 - \frac{m_t - m}{m_t}\xi\right)}{m\xi}}$$

In the third case $\left(\xi > \frac{m_t}{m_t - m}\right)$

$$\frac{\Delta u}{V\alpha}(x,y) = \frac{-2\sigma_s}{\pi\sqrt{m\lambda}} \sqrt{\frac{\xi - 1}{\xi\left(\frac{m_t - m}{m_t}\xi - 1\right)}}\, [KE(k',\psi_3) - (K - E)F(k',\psi_3)] \quad (44c)$$

where

$$\psi_3 = \sin^{-1} \sqrt{\frac{\frac{m_t - m}{m_t}\xi - 1}{\xi - 1}}$$

Along the Mach line from the leading-edge tip, all three equations reduce to the value

$$\frac{\Delta u^*}{V\alpha} = \frac{-\sigma_s}{\sqrt{m\lambda\xi}} \quad (45)$$

By the procedure just described, approximate cancellation of all pressure differences outboard of the tip has been effected, but the pressures induced by such cancellation now violate the condition of zero lift in the wake. Cancellation of the induced pressure differences in the wake can be accomplished in an approximate manner, as in reference 1, by making use of the known value of the induced pressure at the trailing edge of the wing, but assuming the entire error to originate at the tip leading edge.

On the trailing edge of an untapered wing, $\xi = 1$ and

$$\left(\frac{\Delta u}{V\alpha}\right)_{\xi=1} = \frac{-2\sigma_s}{\pi\sqrt{m\lambda}}\, k'K \qquad (46)$$

There is no corresponding simplification for the tapered wing.

The constant-velocity elements to be superposed in cancellation of this tip-induced velocity will be defined by rays of slope t_m/β from the leading-edge tip. (See sketch.) Their apexes will be at the intersection x_t, y_t of the rays with the trailing edge, and they will be bounded by the rays t_m on one side and the trailing edge on the other. The initial sector, bounded by the tip Mach line $t_m = -1$ will have the constant velocity Δu^* given by equation (45). The total induced correction to the velocity at any point x,y will be

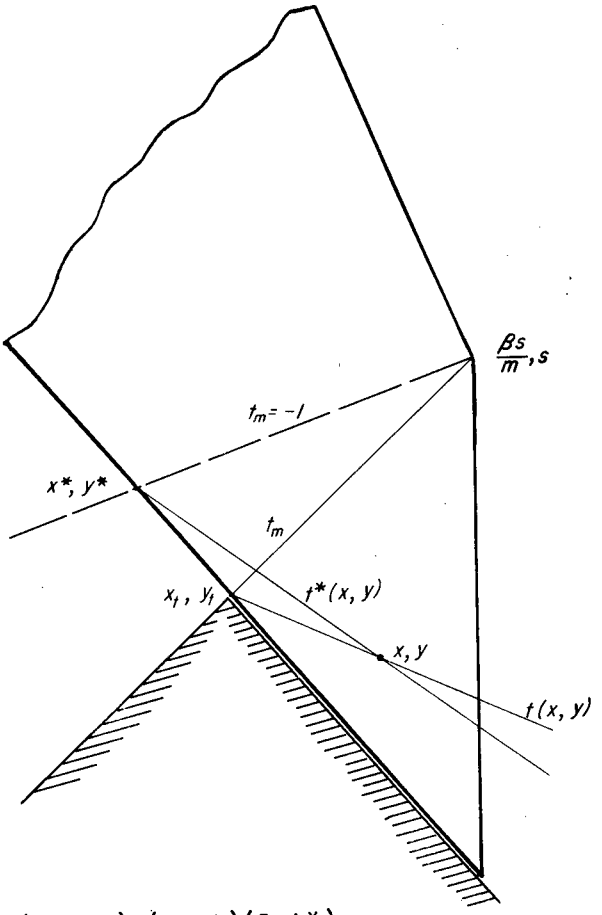

$$\Delta_2 u(x,y) = -\frac{1}{\pi}\cdot\left[\Delta u^* \cos^{-1}\frac{2(t^*-m_t)-(m_t+1)(1-t^*)}{(1-m_t)(t^*+1)} + \int_1^{t=1}\frac{d\Delta u}{dt_m}\cos^{-1}\frac{(1-t_m)(t-m_t)-(m_t-t_m)(1-t)}{(1-m_t)(t-t_m)}\,dt_m\right] \qquad (47)$$

where, if x^*,y^* are the coordinates of the intersection of the tip Mach line with the trailing edge,

$$t^* = \frac{\beta(y-y^*)}{x-x^*} \tag{48}$$

and

$$t = \frac{\beta(y-y_t)}{x-x_t} \tag{49}$$

The integral in equation (47) is most conveniently evaluated by plotting the inverse cosine against Δu, obtained from equation (46) for the untapered wing, or equations (44b) or (44c) for the tapered wing, for the points x_t, y_t on the trailing edge. The two functions are related through t_m, which is defined by

$$t_m = \frac{\beta(y_t-s)}{x_t - \frac{\beta s}{m}} \tag{50}$$

It is difficult to assess the accuracy of the formulas proposed for calculating the tip losses in the loading since no correct values are available for comparison. In figure 12 two streamwise section load distributions calculated by equations (44) and (47) are compared with those obtained by the simplified conical-flows methods described in Appendix C. The latter calculations are correct along the tip Mach lines, but are known to fall below the correct theoretical value at more rearward points. The tip-induced velocity to be canceled at the trailing edge cannot be calculated with significant accuracy by the approximate method employed, so that no estimate could be made of the load curve within the region affected by such cancellation. The cylindrical-flow approximation probably represents as good an estimate as can be obtained at present of the theoretical load distribution in that region.

CONCLUDING REMARKS

Beyond the spanwise station at which the Mach lines from the trailing-edge apex intersect the leading edge of a swept-back wing, the section loading takes on the general form of the two-dimensional subsonic load distribution. A good approximation to the loading in this region can be obtained by applying an easily calculated correction factor to the two-dimensional flat-plate distribution.

The two-dimensional approximation appears to be in good agreement with the theoretically more accurate loading calculated by the conical-flows method for tapered, as well as untapered, wings. In the case of tapered wings, the proposed method is able to predict the increased

loading in the outboard regions (similar to the effect found in subsonic flow).

The same concept of utilizing two-dimensional loading can be employed to obtain an estimate of the loss of loading in the zone of influence of the wing tip, when the tip lies wholly within the trailing-edge Mach cone. This simplification is especially valuable because even approximate application of the conical-flows method is tedious, and physical conditions of flow in the tip region are so different from the conditions assumed in the theory that a rough indication of the nature of the theoretical load should suffice at the present time as a basis for further investigations.

The approximations of the conical-flows method, as it has been applied herein, should be noted: (1) In canceling lift behind either wing half, a small amount of upwash introduced on the other half of the wing — in violation of the boundary conditions — is ignored and (2), if the trailing-edge Mach line intersects the leading edge, its reflection will intersect the trailing edge and, within the Mach cone from the point of intersection, only an estimate of the loading is feasible. If the next reflection (in the trailing edge) results in a second intersection of the Mach line with the leading edge, the leading-edge correction factor for adjusting the two-dimensional load distribution will also be in error. Calculations made to check the first of these approximations showed the induced-downwash angle to be less than half of 1 percent of the angle of attack on the wings considered. The magnitude of the inaccuracy introduced by the second limitation has been indicated by the examples presented herein; the result is to limit the aspect-ratio Mach number combinations (as expressed by the reduced aspect ratio βA) for which the conical-flows method will give accurate theoretical solutions. The corresponding error in the leading-edge correction coefficient appears, however, to be insignificant and it is felt that, with the exception of wings tapered to a point, the upper range of reduced aspect ratio βA is adequately covered by the proposed method of correcting the two-dimensional load distribution. There remains only the case in which the reduced span (β times the geometric span) is less than the tip chord. In this case, the interference of the tip flows with each other will, in conjunction with a subsonic trailing edge, create a problem not readily solvable by either the conical-flows method or the two-dimensional approximation. This problem falls within the scope of the slender-wing theory of reference 4.

Ames Aeronautical Laboratory,
National Advisory Committee for Aeronautics,
Moffett Field, Calif., Sept. 16, 1949.

APPENDIX A

SYMBOLS

General

V	free-stream velocity
M	free-stream Mach number
β	$\sqrt{M^2-1}$
ρ	density of air
q	dynamic pressure $\left(\frac{1}{2}\rho V^2\right)$
Δp	pressure difference between upper and lower surfaces, or local lift
α	angle of attack, radians
Γ	circulation on infinite flat plate
c	chord of infinite flat plate (See sketch, p. 13.)

Wing Dimensions

c_o	root chord
c_t	tip chord
s	semispan
Λ	angle of sweep of the leading edge
λ	taper ratio (c_t/c_o)

Coordinates

x,y	Cartesian coordinates in the stream direction and across the stream in the plane of the wing
x_a,y_a	coordinates of apex of oblique trailing-edge element
x_b,y_b	coordinates of apex of leading-edge element
x_t,y_t	coordinates of point on trailing edge, within tip Mach cone

x_c streamwise coordinate of apex of tip element

x_o largest value of x_c at which cancellation of pressure can affect point at which pressure is being calculated

ξ streamwise distance of x,y back from leading edge, as a fraction of the tip chord (equation (40))

ξ_c distance of x_c behind leading-edge tip, as a fraction of the tip chord (equation 34))

ξ_o distance of x_o behind leading-edge tip, as a fraction of the tip chord (equation (41))

η spanwise distance of x,y from leading edge, as a fraction of the chord through x,y measured perpendicular to the stream (equation (28))

In the following, all slopes are measured counterclockwise from a line extending downstream from the apex of the wing or of the pertinent elementary sector:

m $\dfrac{\text{slope of leading edge}}{\text{slope of Mach lines}} = \beta \cot \Lambda$

m_t $\dfrac{\text{slope of trailing edge}}{\text{slope of Mach lines}}$

a $\dfrac{\text{slope of ray from the origin}}{\text{slope of Mach lines}} = \beta \dfrac{y}{x}$

t_o $\dfrac{\text{slope of ray from trailing-edge apex}}{\text{slope of Mach lines}} = \beta \dfrac{y}{x-c_o}$

t_m $\dfrac{\text{slope of ray from leading-edge tip}}{\text{slope of Mach lines}} = \beta \dfrac{y-s}{x-(\beta s/m)}$

t_a $\dfrac{\text{slope of ray from apex of element a}}{\text{slope of Mach lines}} = \beta \dfrac{y-y_a}{x-x_a}$

t_b $\dfrac{\text{slope of ray from apex of leading-edge element}}{\text{slope of Mach lines}} = \beta \dfrac{y-y_b}{x-x_b}$

t_b^* t_b for point at which pressure is being calculated

t_c $\dfrac{\text{slope of ray from apex of tip element}}{\text{slope of Mach lines}} = \beta \dfrac{y-s}{x-x_c}$

a_o the value of a corresponding to a trailing-edge element of which the apex lies on the Mach forecone of the point at which the load is being calculated

a_o' the largest value of a along which cancellation of pressure in the wake can affect the point at which the load is being calculated through reflection in the leading edge

τ_o the smallest value of t_o along which cancellation of pressure ahead of the leading edge can affect the point at which pressure is being calculated (equation (11))

τ_a the smallest values of t_a along which cancellation of pressure ahead of the leading edge can affect the point at which pressure is being calculated (equation (16))

Streamwise Components of Perturbation Velocity

u_Δ basic (uncorrected) perturbation velocity as given by solution for triangular wing (equation (1))

u_o value of u_Δ at a=0 (equation (2))

u_a constant perturbation velocity on canceling (oblique) sector in wake

u_b constant perturbation velocity on canceling sector ahead of wing

u_c constant perturbation velocity on canceling sector outboard of tip

$(\Delta u)_o$ symmetrical trailing-edge correction to u_Δ (equation (3))

$(\Delta u)_a$ correction to u_Δ due to single oblique trailing-edge element $\left(\frac{d\Delta u}{da}\,da\right)$

$(\Delta u)_b$ leading-edge correction to u_Δ

$(\Delta u_b)_o$ leading-edge correction to u_Δ due to reflection of $(\Delta u)_o$ (equation (10))

$(\Delta u)_c$ correction to u_Δ due to reflection of leading-edge correction in wing tip (terms in R only)

$\Delta_2 u$ perturbation velocity induced by canceling tip effect at the trailing edge (equation (47))

Arbitrary Mathematical Symbols

r.p.	real part
R	radical term of leading-edge correction function (equation (9))
C	inverse-cosine term of leading-edge correction function (equation (8))
C_Δ	value of coefficient of $(mx-\beta y)^{-1/2}$ in u_Δ at the leading edge (strength of the leading-edge singularity in u)
$(\Delta C)_o$	decrement in the strength of the leading-edge singularity in u due to reflection of $(\Delta u)_o$ at leading edge
$\frac{d\Delta C}{da}da$	decrement in the strength of the leading-edge singularity in u due to reflection of $(\Delta u)_a$ at leading edge
σ	leading-edge correction coefficient defined by equation (25)
σ_s	value of σ at leading-edge tip

Elliptic Integrals (See references 5 and 6.)

k	modulus of elliptic integral (defined where used)
k'	the complementary modulus $(\sqrt{1-k^2})$
φ or ψ	argument of elliptic integrals (defined where used)
$F(k,\varphi)$	incomplete elliptic integral of the first kind of modulus k and argument φ
K,K(k)	complete elliptic integral of the first kind of modulus k $[K = F(k,\frac{\pi}{2})]$
$E(k,\varphi)$	incomplete elliptic integral of the second kind
E,E(k)	complete elliptic integral of the second kind of modulus k $[E = E(k,\frac{\pi}{2})]$
K'(k)	K of the complementary modulus $[K'(k) = K(k')]$

APPENDIX B

EVALUATION OF $\int_{\tau_o}^{1} \frac{d(\Delta u)_o}{dt_o} C(t_o)dt_o$ BY SERIES EXPANSION

For integration of the first term of equation (10), the product $[d(\Delta u)_o/dt_o]\, C(t_o)$ is integrated by parts to give

$$\int_{\tau_o}^{1} \frac{d(\Delta u)_o}{dt_o} C(t_o)dt_o = (\Delta u)_o\, C(t_o)\Big|_{\tau_o}^{1} - \int_{\tau_o}^{1} (\Delta u)_o \frac{dC(t_o)}{dt_o}\, dt_o \qquad (B1)$$

The first term goes to zero at either limit. In the second term, t_b must be expressed in terms of x, y, and t_o before taking the derivative of $C(t_o)$. If the constant (for any selected point)

$$t_o^* = \frac{\beta y}{x - c_o}$$

is defined, this derivative may be written

$$\frac{dC(t_o)}{dt_o} = \frac{(1+t_o^*)\sqrt{(\tau_o - m)(mx - \beta y)}}{(t_o - t_o^*)\sqrt{mc_o(1+m)(1+t_o)(t_o - \tau_o)}} \qquad (B2)$$

If this expression and the expression for $(\Delta u)_o$ given by equation (3) are substituted in equation (B1), the result

$$\int_{\tau_o}^{1} \frac{d(\Delta u)_o}{dt_o} C(t_o)dt_o = \frac{u_o(1+t_o^*)}{K(\sqrt{1-m_t^2})} \sqrt{\frac{(\tau_o - m)(mx - \beta y)}{mc_o(1+m)}} \times \int_{\tau_o}^{1} \frac{F(\sqrt{1-m_t^2},\, \varphi)}{(t_o - t_o^*)\sqrt{(1+t_o)(t_o - \tau_o)}}\, dt_o \qquad (B3)$$

is obtained. For t_o close to 1 (small values of φ), $F(\sqrt{1-m_t^2},\varphi)$ may be expanded into a MacLauren series in $\sin\varphi = \sqrt{(1-t_o^2)/(1-m_t^2)}$ as follows:

$$F\left(\sqrt{1-m_t^2},\varphi\right) = \sqrt{\frac{1-t_o^2}{1-m_t^2}} + \frac{1+(1-m_t^2)}{6}\left(\frac{1-t_o^2}{1-m_t^2}\right)^{3/2} + \frac{3+2(1-m_t^2)+3(1-m_t^2)^2}{40}\left(\frac{1-t_o^2}{1-m_t^2}\right)^{5/2} + \cdots \tag{B4}$$

From the first two terms of the series, substituted in equation (B3), we may obtain

$$\int_{\tau_o}^{1}(u_b)_o\, C(t_o)dt_o = \frac{\pi u_o(1+t_o^*)}{K\left(\sqrt{1-m_t^2}\right)}\sqrt{\frac{(\tau_o-m)(mx-\beta y)}{mc_o(1+m)(1-m_t^2)}}\left\{\left(\sqrt{\frac{1-t_o^*}{\tau_o-t_o^*}}-1\right)\left[1+\frac{1}{6}\left(1+\frac{1}{1-m_t^2}\right)(1-t_o^{*2})\right]-\frac{1-\tau_o}{48}\left(1+\frac{1}{1-m_t^2}\right)(1+3\tau_o+4t_o^*)\right\} \tag{B5}$$

The corresponding expression has been derived for $\int(u_b)_a C(t_a)dt_a$, but the results are numerically insignificant in most cases.

APPENDIX C

CALCULATION OF TIP LOSS IN LOADING BY CONICAL-FLOWS METHOD

If the trailing-edge Mach line intersects the leading edge on the wing, four components of the perturbation velocity, as calculated by the conical-flows method, must be canceled outboard of the tip:[3] (1) the basic velocity u_Δ, (2) the trailing-edge correction $(\Delta u)_o + \int_o^{a_o} \frac{d\Delta u}{da}\,da$, (3) the leading-edge corrections $(\Delta u)_b = (\Delta u_b)_o + \int_o^{a_o'} \frac{d(\Delta u)_b}{da}\,da$, and (4) the reflection of $(\Delta u)_b$ in the trailing edge (in region IV, fig. 1). This last component has not been calculated. If it does not extend over more than 50 percent of the tip section, the effect of its cancellation at the tip can probably be neglected.

The third component $(\Delta u)_b$ can be further broken down into the parts arising from the radical term R in the leading-edge correction function and those arising from the inverse-cosine term C. The former components increase to infinity at the leading edge and will be treated in the same way as the basic velocity u_Δ. The latter remain finite and exactly cancel the trailing-edge corrections $(\Delta u)_o + \int_o^{a_o} \frac{d\Delta u}{da}\,da$ at the leading edge of the tip section. Although these components (the C component of $(\Delta u)_b$, and the trailing-edge correction) do not cancel each other elsewhere on the tip section or in the stream, the variation of each is fairly small in the region affecting the pressures on the wing, and, since the net induced effect of canceling them is zero and has zero slope along the tip Mach cone, it will be assumed that they cancel each other completely. This assumption will result in somewhat too low a loading near the trailing edge.

Cancellation of the first component, the basic velocity u_Δ, has been covered in reference 1. The result is a reduction in u given by

$$\Delta u = \frac{u_o\sqrt{m}}{\pi}\left\{\sqrt{\frac{2\beta(s-y)}{x+\beta y}}\,K - 2x\sqrt{\frac{m}{m^2x^2-\beta^2y^2}}\left[\frac{F(k',\psi)}{K'}\left(\frac{\pi}{2}-KE'\right)+KE(k',\psi)\right]\right\} \tag{C1}$$

[3] If the tip lies beyond region IV (fig. 1) further small components enter, but these will not be considered in the present analysis.

(equation (37) of reference 1), where s is the semispan,

$$k = \sqrt{\frac{(m-a_o)(1-m)}{2m(a_o+1)}},$$

$$\psi = \sin^{-1}\sqrt{\frac{a_o(mx+\beta y)}{\beta s(a_o+m)}},\quad a_o = \frac{\beta s}{x+\beta(y-s)},$$

$K' = K(k')$, and $E' = E(k')$.

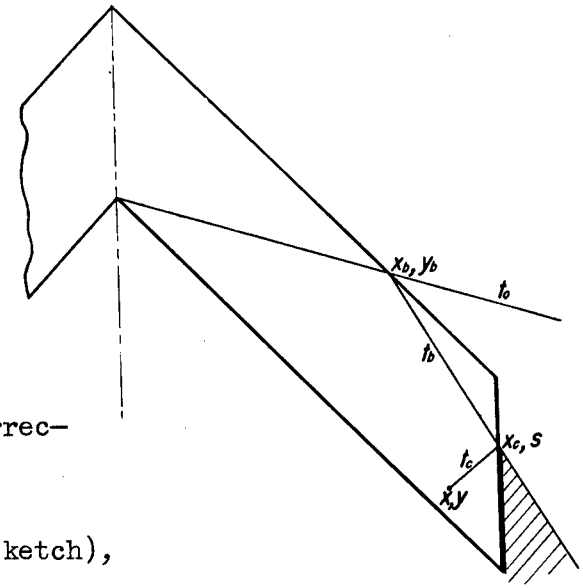

The part of the leading-edge correction associated with $R(t_o)$ may be canceled by the following procedure:

For any one value of t_o (see sketch), the correction to $u(x,y)$ will be

$$\frac{d(\Delta u)_c}{dt_o}\,dt_o = -\frac{1}{\pi^2}\frac{d(\Delta u)_o}{dt_o}\,dt_o \operatorname*{limit}_{t_b \to m}\left[R(t_o,t_b)\cos^{-1}\frac{t_b+t_c+2t_bt_c}{t_c-t_b} + \int_{t_b}^{t_c=-1}\frac{\partial R}{\partial t_b}\cos^{-1}\frac{t_b+t_c+2t_bt_c}{t_c-t_b}\,dt_b\right] \tag{C2}$$

where $t_b = \frac{\beta(s-y_b)}{x_c-x_b}$ (see sketch).

Integrating by parts results in the elimination of the first term so that

$$\frac{d(\Delta u)_c}{dt_o}\,dt_o = \frac{1}{\pi^2}\frac{d(\Delta u)_o}{dt_o}\,dt_o \int_m^{t_c=-1} R(t_o,t_b)\frac{d}{dt_b}\cos^{-1}\frac{t_b+t_c+2t_bt_c}{t_c-t_b}\,dt_b \tag{C3}$$

Equation (C3) can be integrated analytically, giving

$$\frac{d(\Delta u)_c}{dt_o}\,dt_o = \frac{2m}{\pi(1+m)t_o}\sqrt{\frac{(t_o-m)(1+t_o)(1+t_b^*)}{m-t_b^*}}\,d(\Delta u)_o \tag{C4}$$

where

$$t_b^* = \frac{\beta(y-y_b)}{x-x_b}$$

To obtain the total correction to $u(x,y)$ for the cancellation of the term in $R(t_o)$ of the leading-edge correction, equation (C4) may be integrated graphically by plotting against $(\Delta u)_o$ the remainder of the expression in the right-hand side. An approximate correction for the reflection of the terms in $R(t_a)$ can be included by plotting against the values of

$$\Delta u = (\Delta u)_o + \int_o^{a_o} \frac{d\Delta u}{da}\, da$$

along the leading edge. Then

$$(\Delta u)_c = \frac{2m}{\pi(1+m)} \int_{t_o=1}^{t_b^*=-1} \frac{1}{t_o} \sqrt{\frac{(t_o-m)(1+t_o)(1+t_b^*)}{m-t_b^*}}\, d\Delta u \qquad (C5)$$

where t_o, t_b^*, and Δu are all computed for specified locations of x_b, y_b on the leading edge and the extension of the leading edge to the point such that $t_b^* = -1$.

In practice, equation (C5) appears to result in a nearly constant correction to the section loading, as shown in figures 12(a) and (b). The work may be further simplified, therefore, by performing only the relatively simple calculation for a point on the Mach line.

REFERENCES

1. Cohen, Doris: The Theoretical Lift of Flat Swept-Back Wings at Supersonic Speeds. NACA TN 1555, 1948.

2. Lagerstrom, P. A.: Linearized Supersonic Theory of Conical Wings. NACA TN 1685, 1948.

3. Goodman, Theodore R.: The Lift Distribution on Conical and Non-Conical Flow Regions of Thin Finite Wings in a Supersonic Stream. Jour. of the Aero. Sci., Vol. 16, No. 6, June, 1949, pp. 365 - 374.

4. Heaslet, Max. A., Lomax, Harvard, and Spreiter, John R.: Linearized Compressible-Flow Theory for Sonic Flight Speeds. NACA TN 1824, 1949.

5. Peirce, B. O.: A Short Table of Integrals. Ginn and Company (Boston), 1929, pp. 66 and 121 - 123.

6. Legendre, Adrien Marie: Tables of the Complete and Incomplete Elliptic Integrals. Biometrika Office, University College, Cambridge University Press, Cambridge, England, 1934.

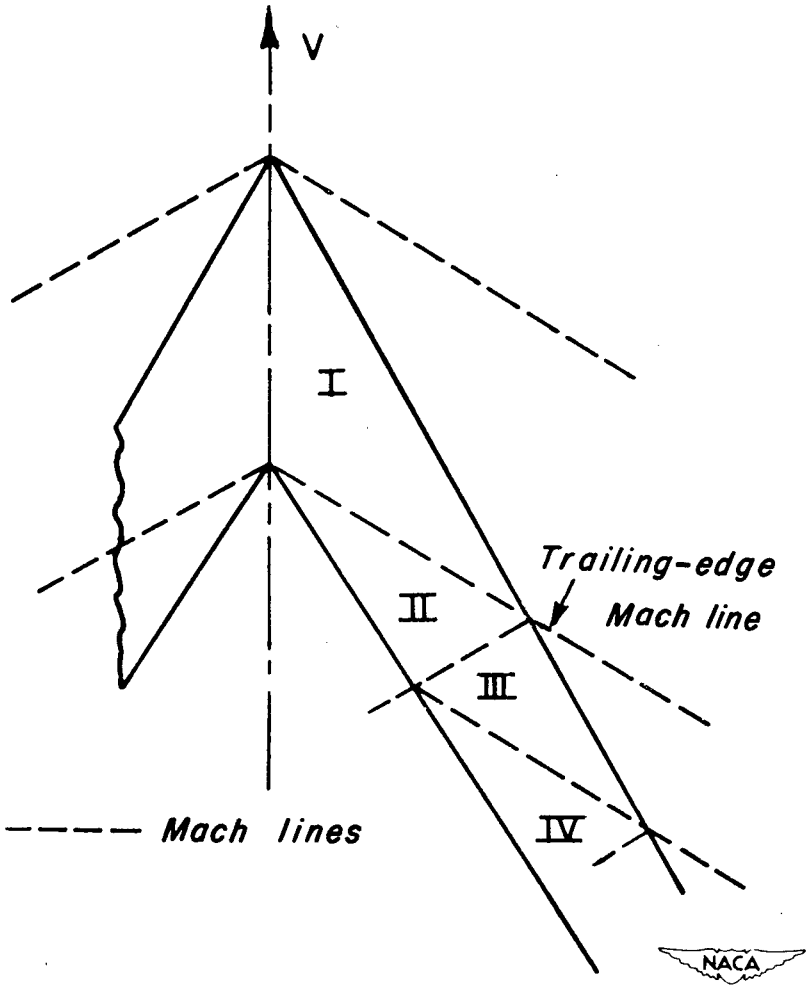

Figure 1. – Plan view of central portion of swept-back wing showing pattern of Mach lines arising at leading and trailing edges.

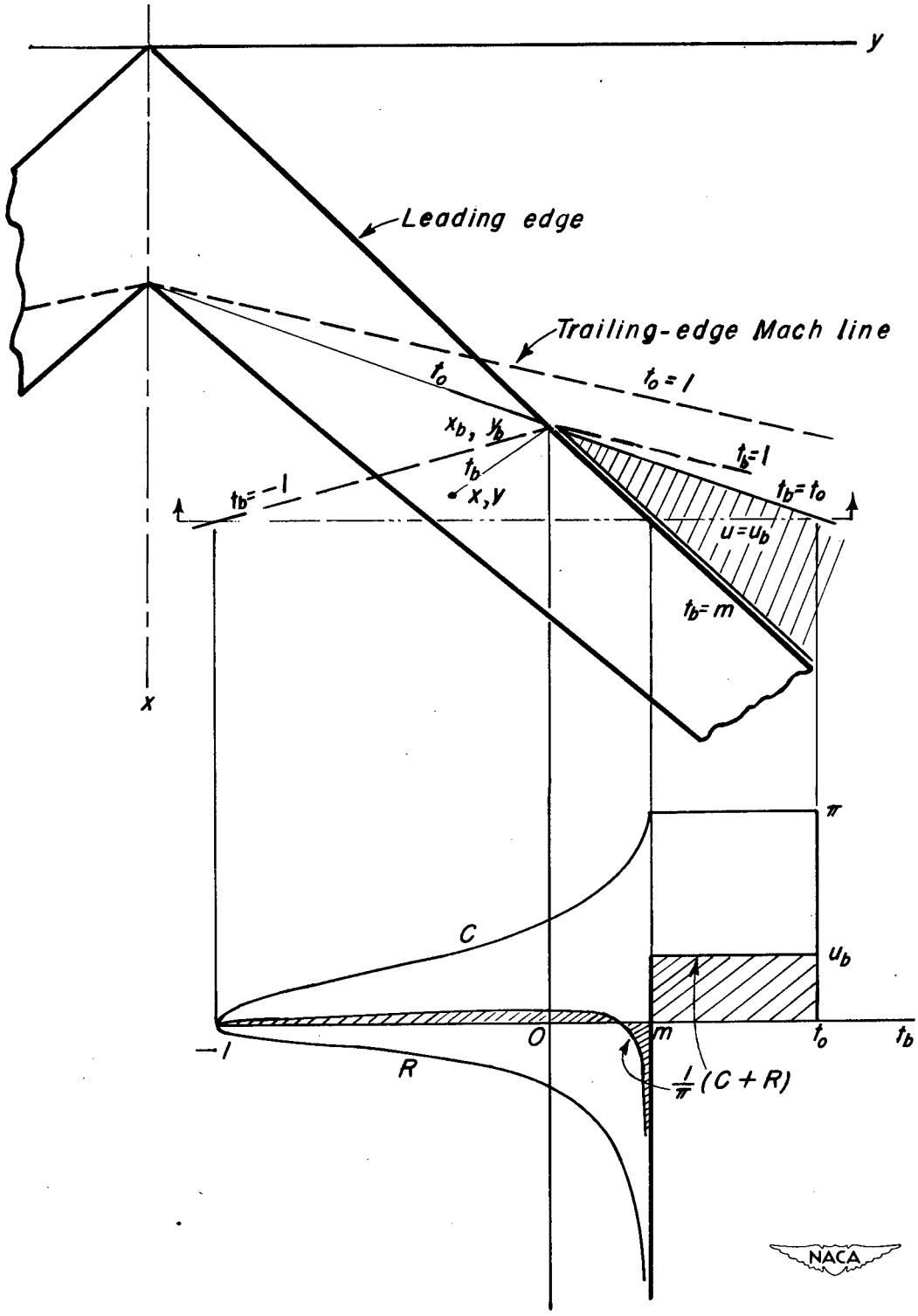

Figure 2. — Leading-edge element and induced-velocity function.

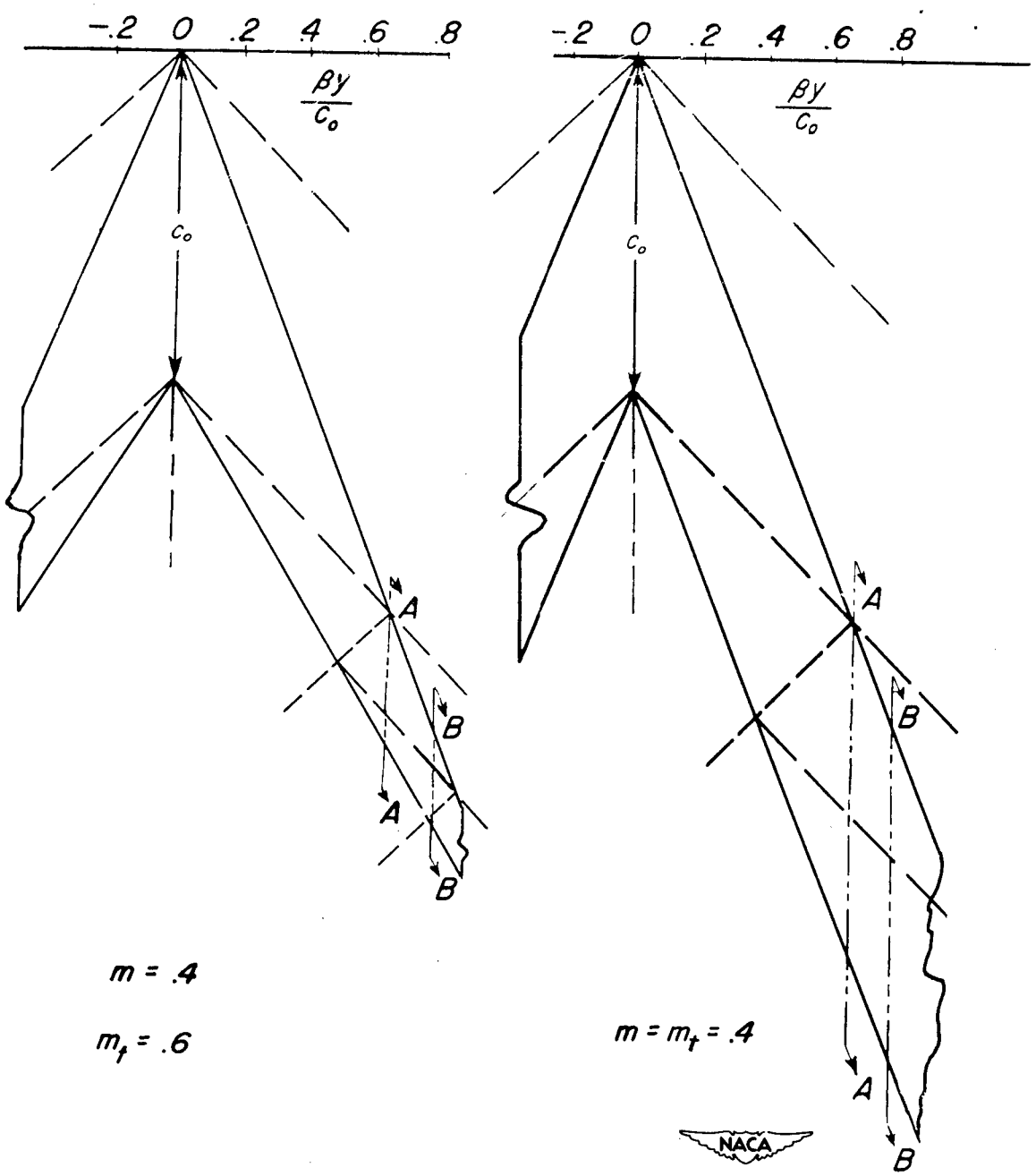

Figure 3.– Plan view of tapered and untapered wings, m = 0.4, showing Mach line patterns and sections of which lift distributions were calculated.

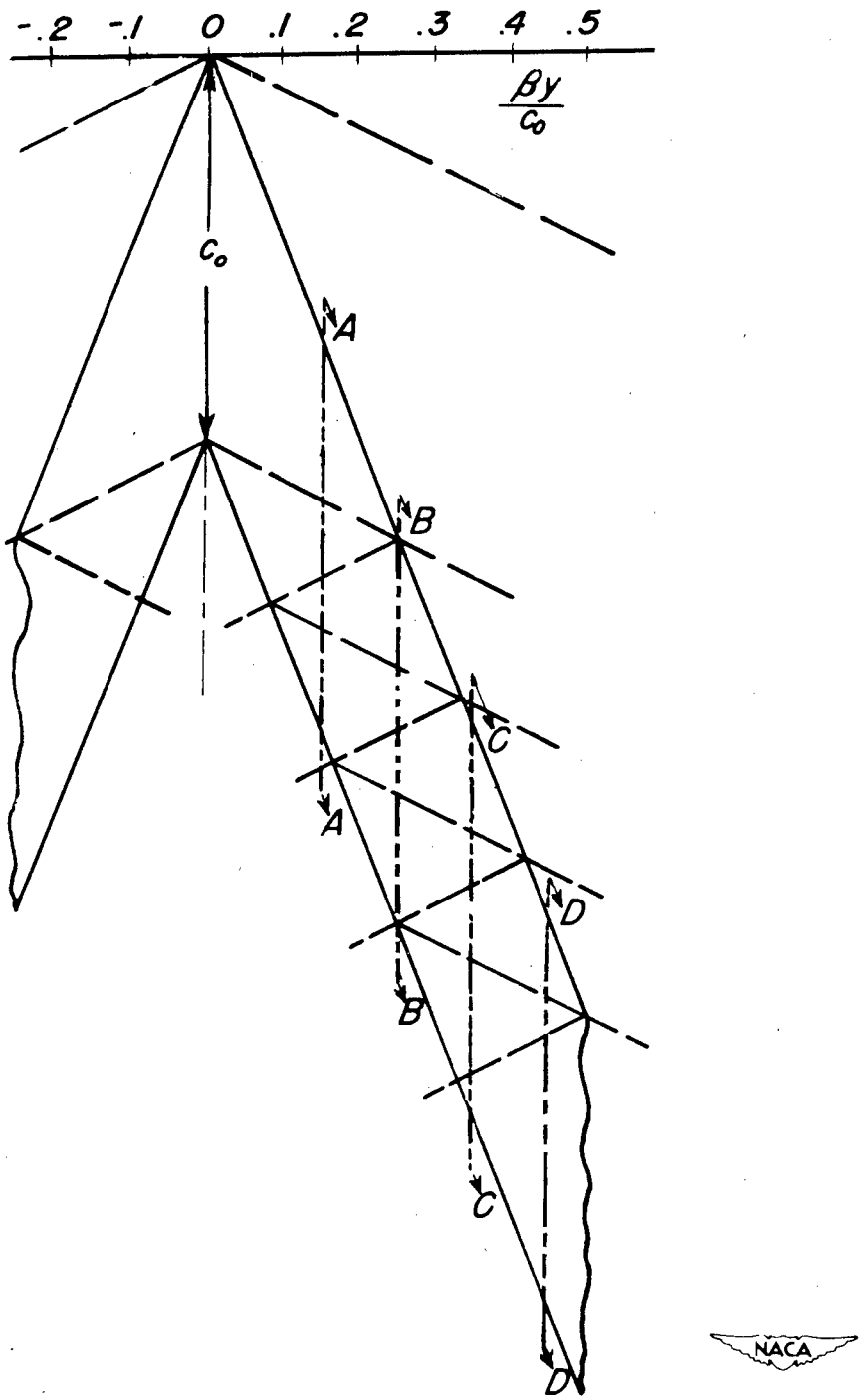

Figure 4. — Plan view of untapered wing, m = 0.2, showing Mach line pattern and sections at which lift distributions were calculated.

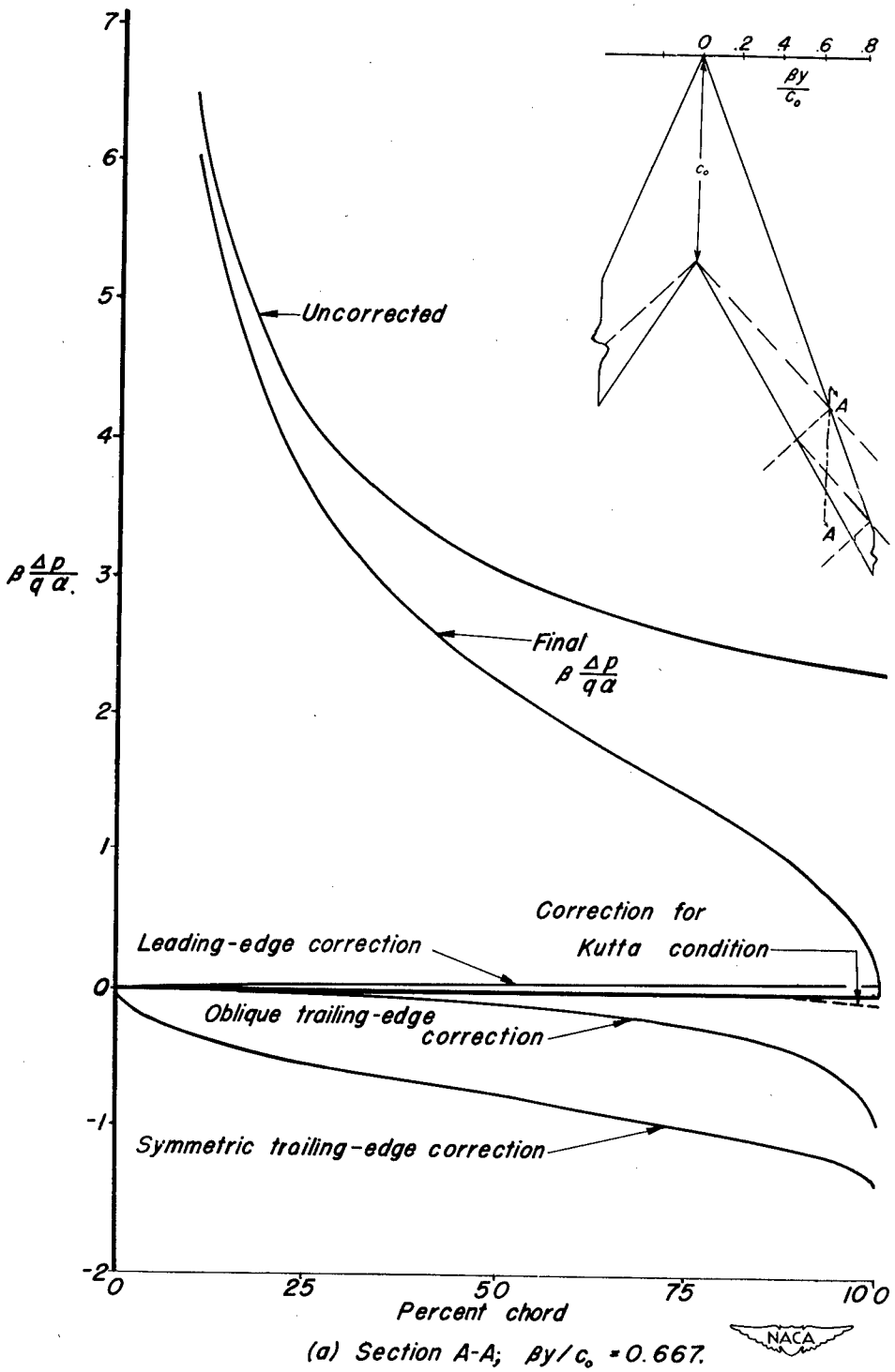

(a) Section A-A; $\beta y/c_o = 0.667$.

Figure 5. - Load distribution over two streamwise sections of the tapered swept-back wing calculated by the conical-flows method.

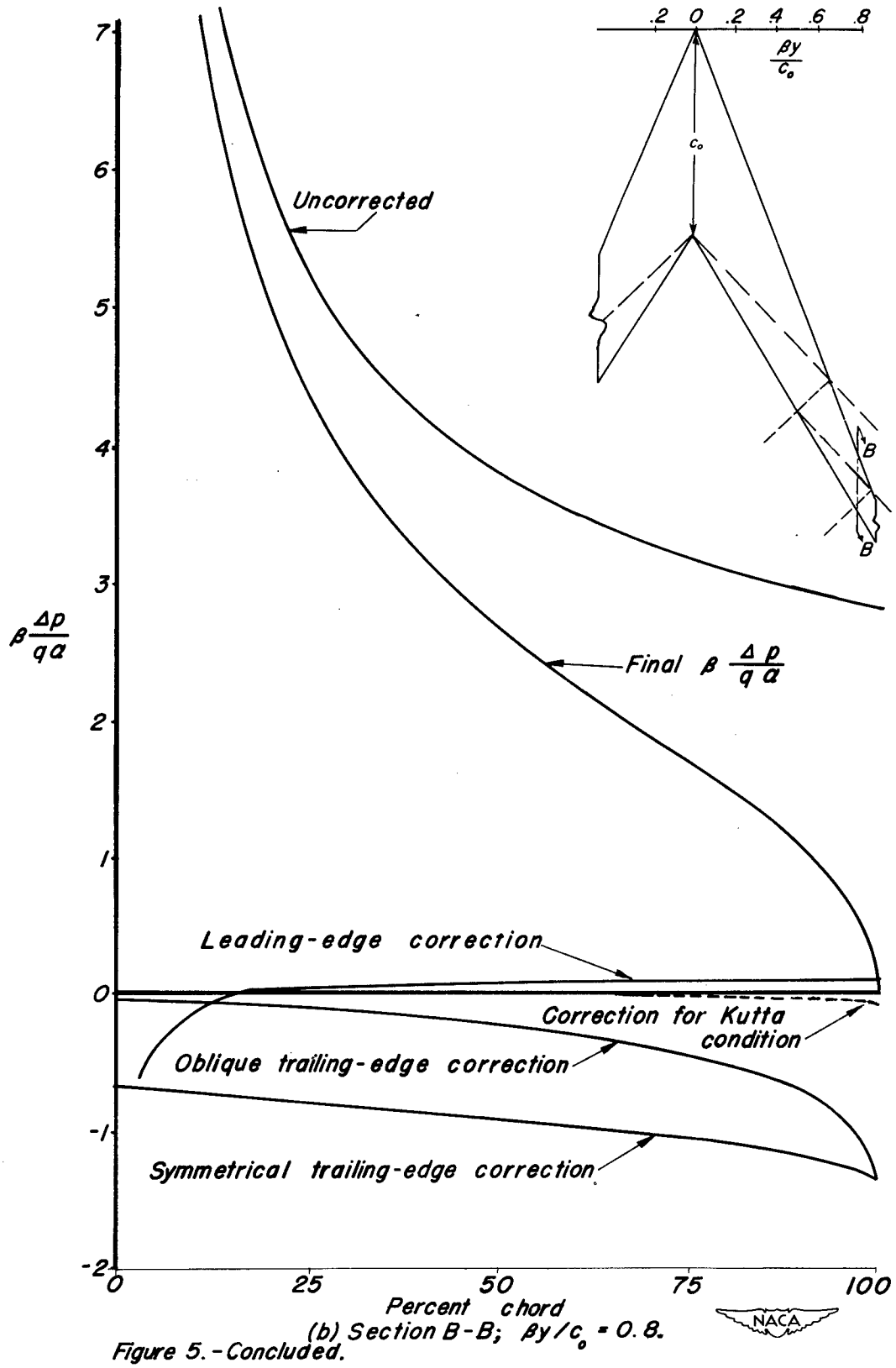

(b) Section B-B; $\beta y/c_0 = 0.8$.

Figure 5.- Concluded.

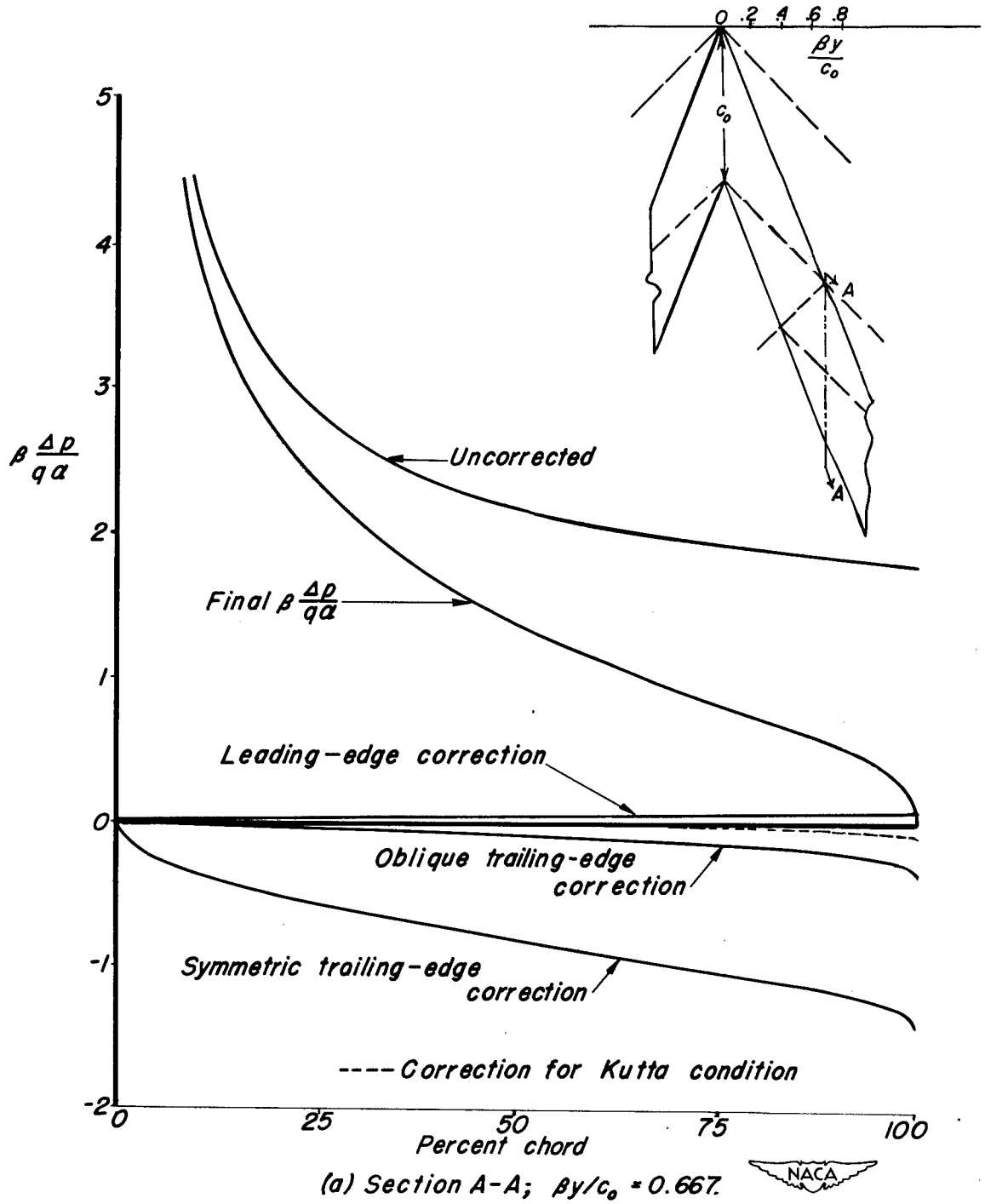

(a) Section A-A; $\beta y/c_o = 0.667$.

Figure 6.- Load distribution over two streamwise sections of the untapered swept-back wing, m = 0.4, calculated by the conical-flows method.

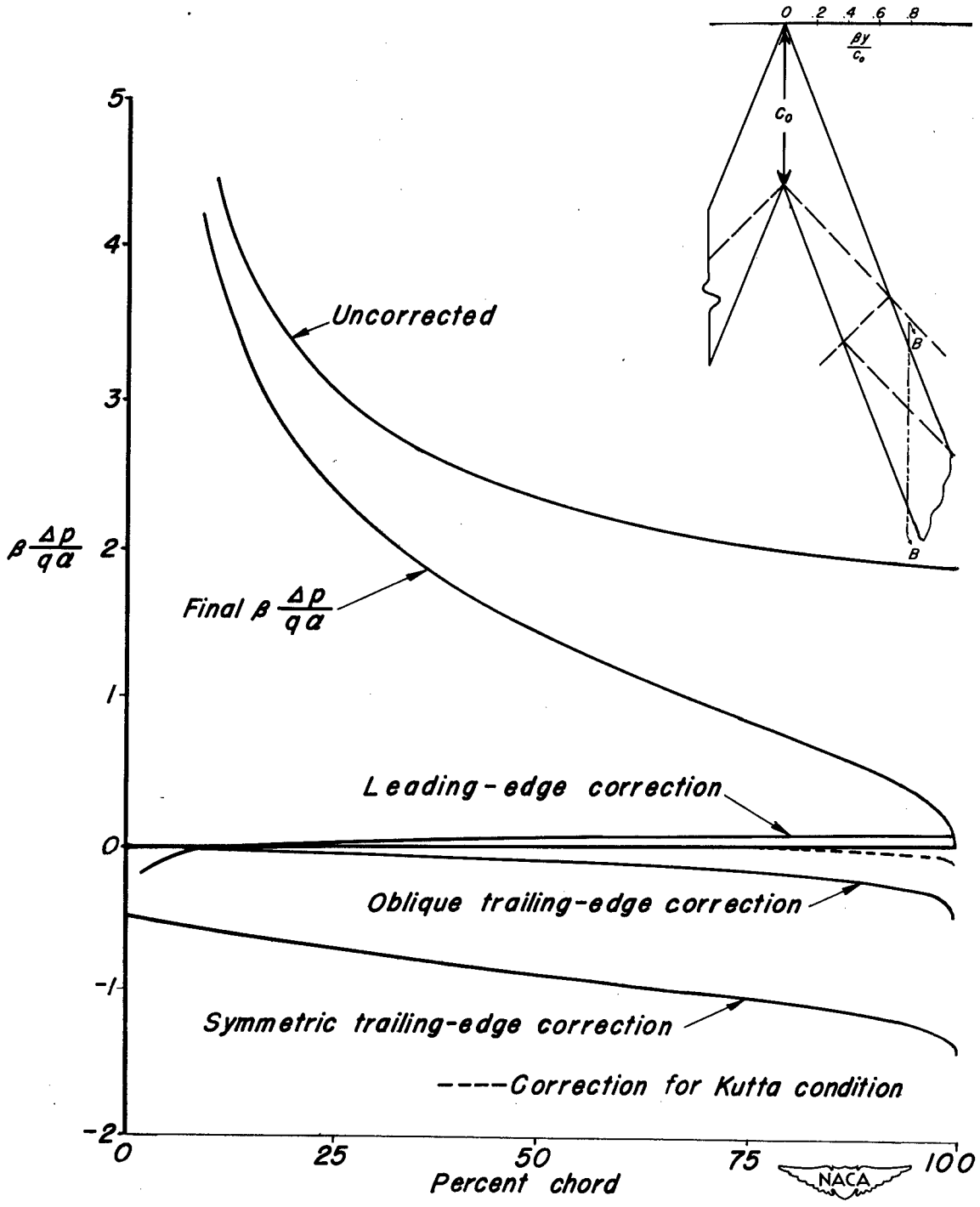

(b) Section B-B; $\beta y / c_0 = 0.8$.

Figure 6. - Concluded.

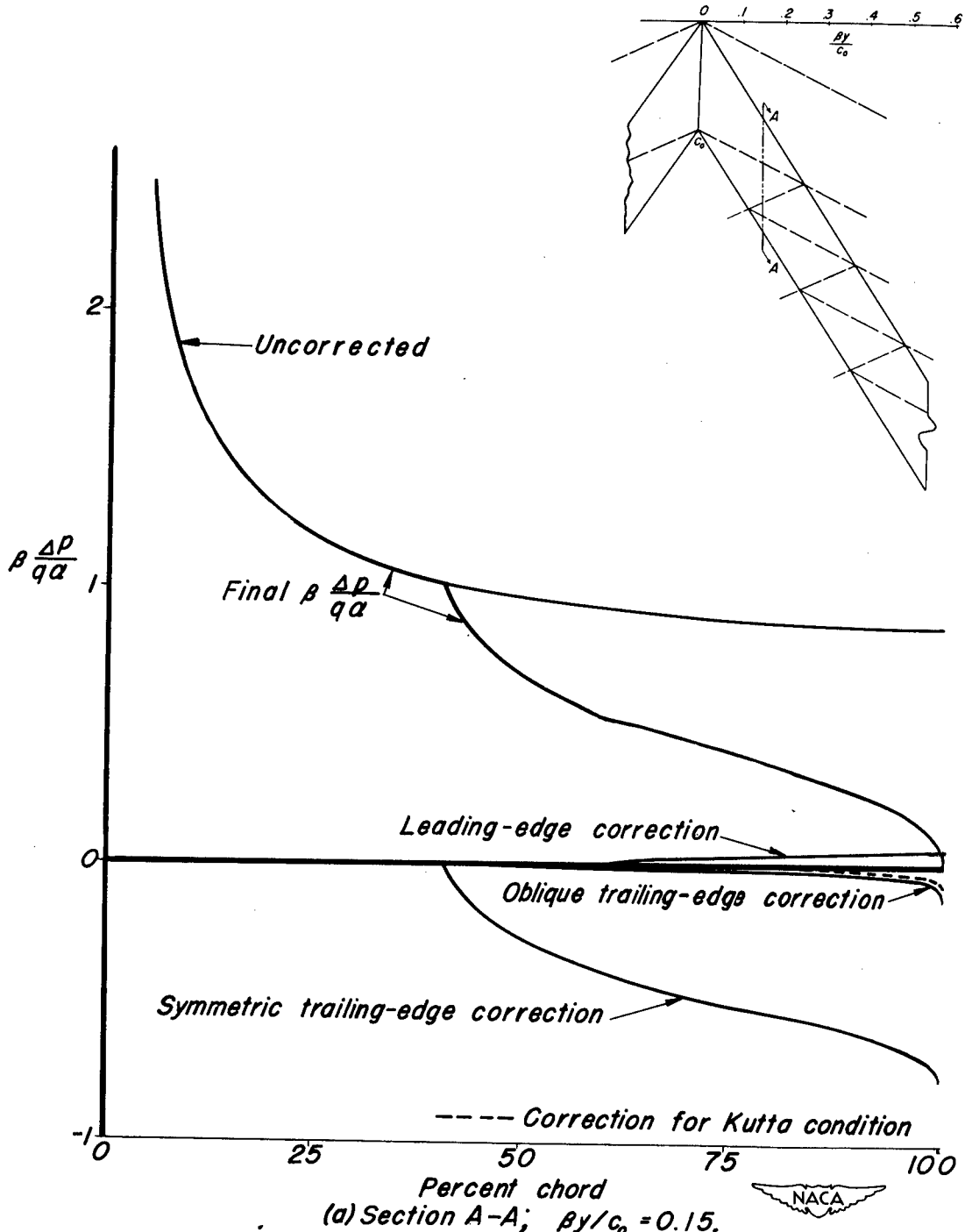

(a) Section A-A; $\beta y/c_0 = 0.15$.

Figure 7. – Load distributions over four streamwise sections of the untapered swept-back wing, m=0.2, calculated by the conical-flows method.

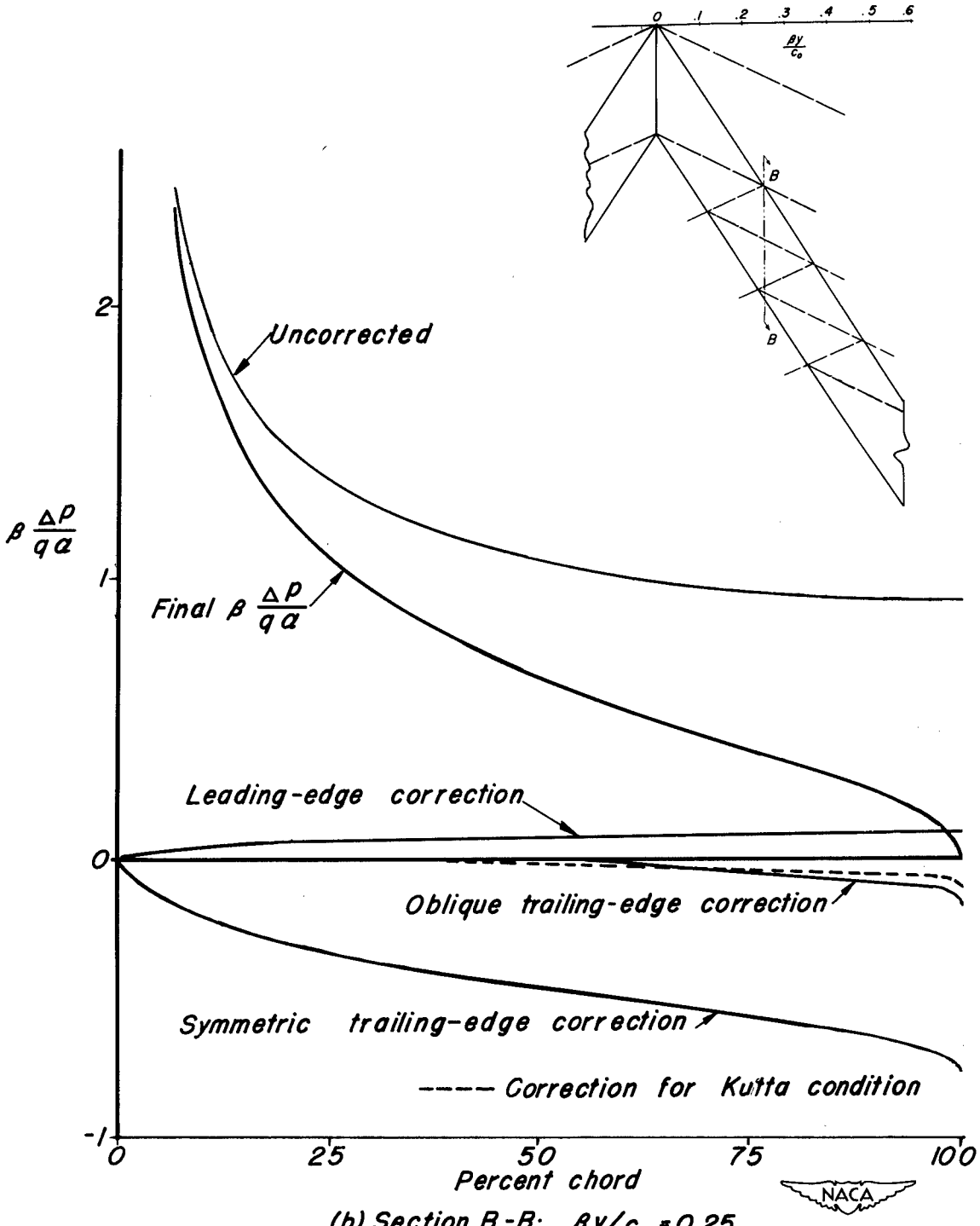

(b) Section B-B; $\beta y/c_0 = 0.25$.

Figure 7.- Continued.

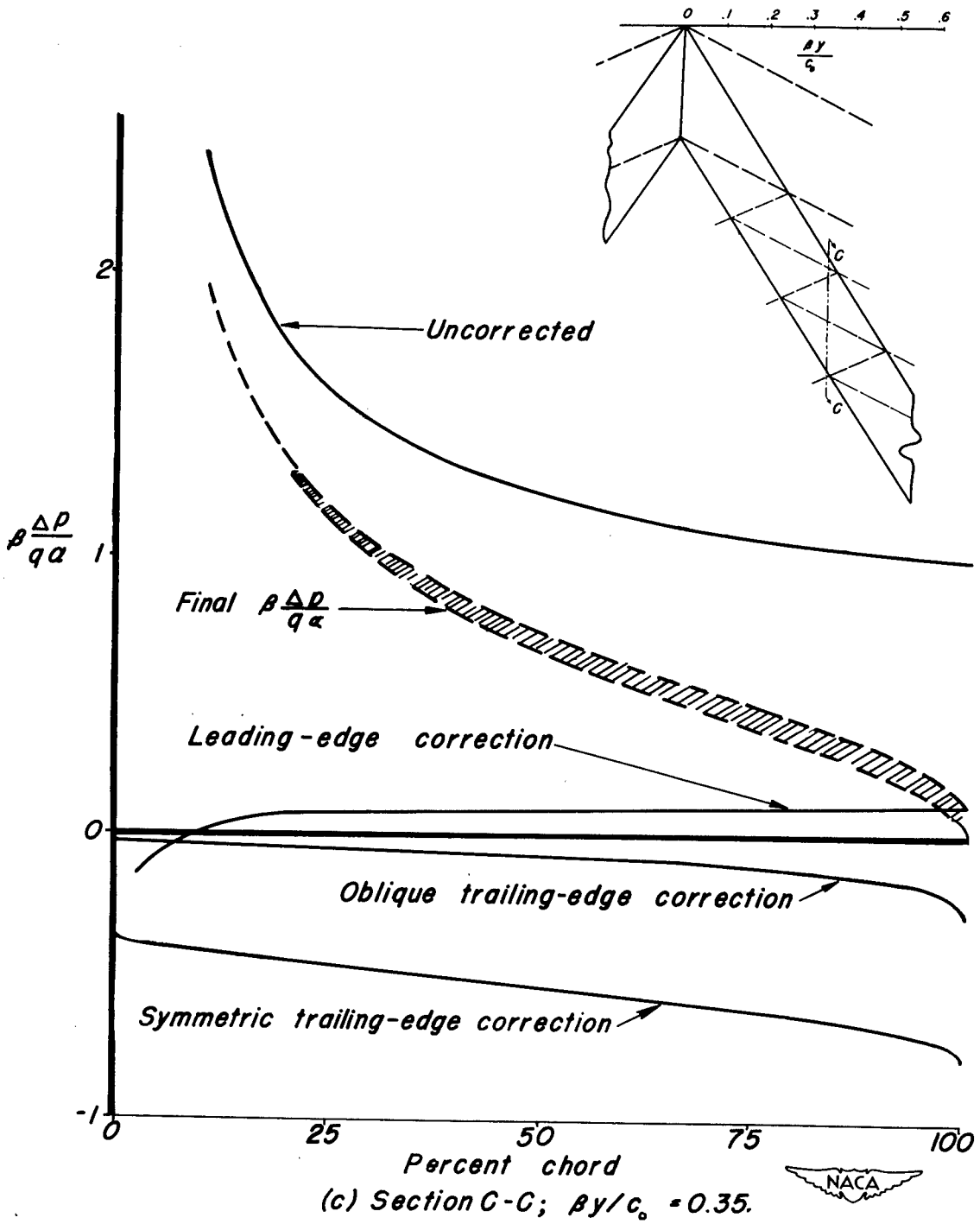

(c) Section C-C; $\beta y / c_0 = 0.35$.

Figure 7.- Continued.

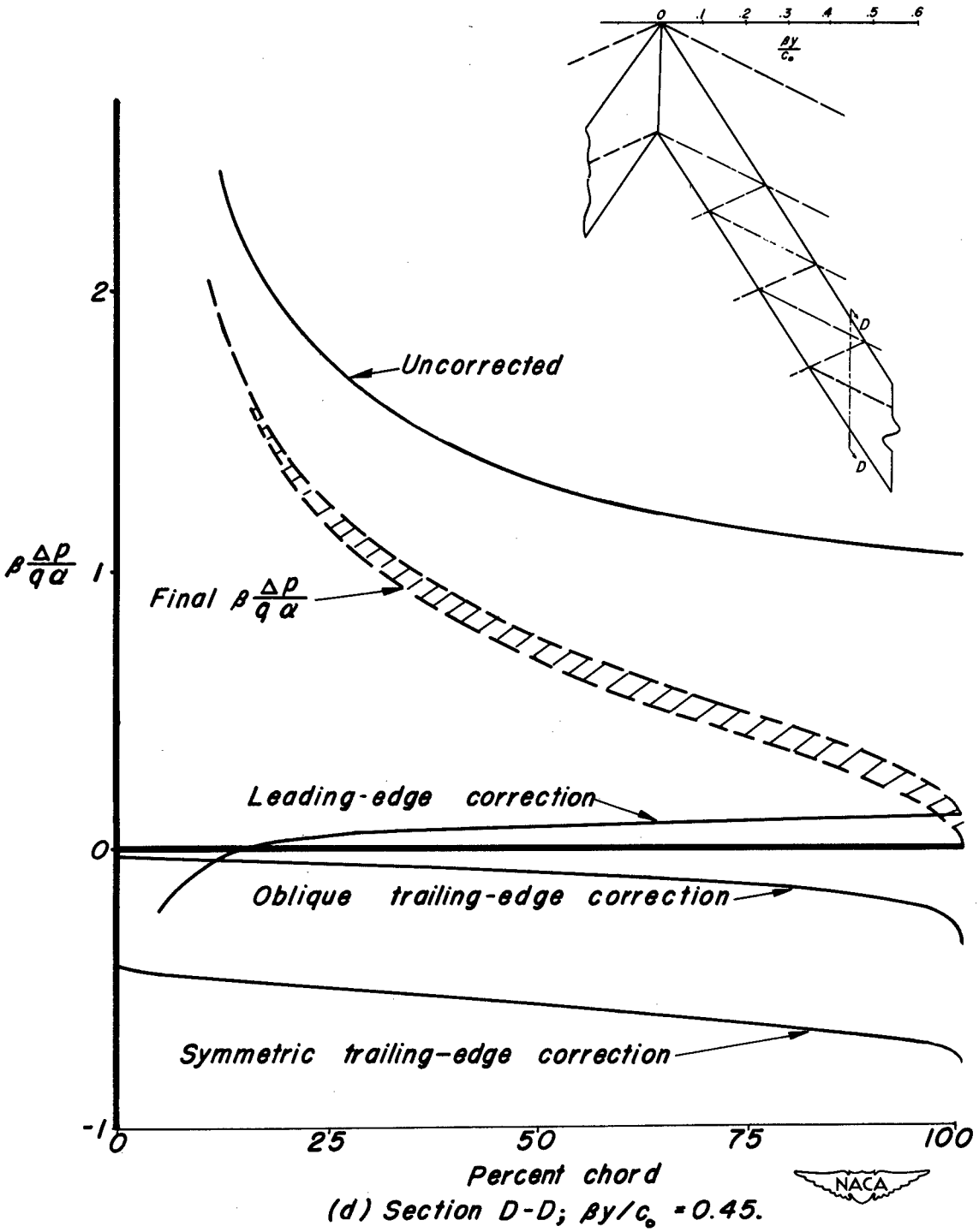

(d) Section D-D; $\beta y/c_0 = 0.45$.

Figure 7.- Concluded.

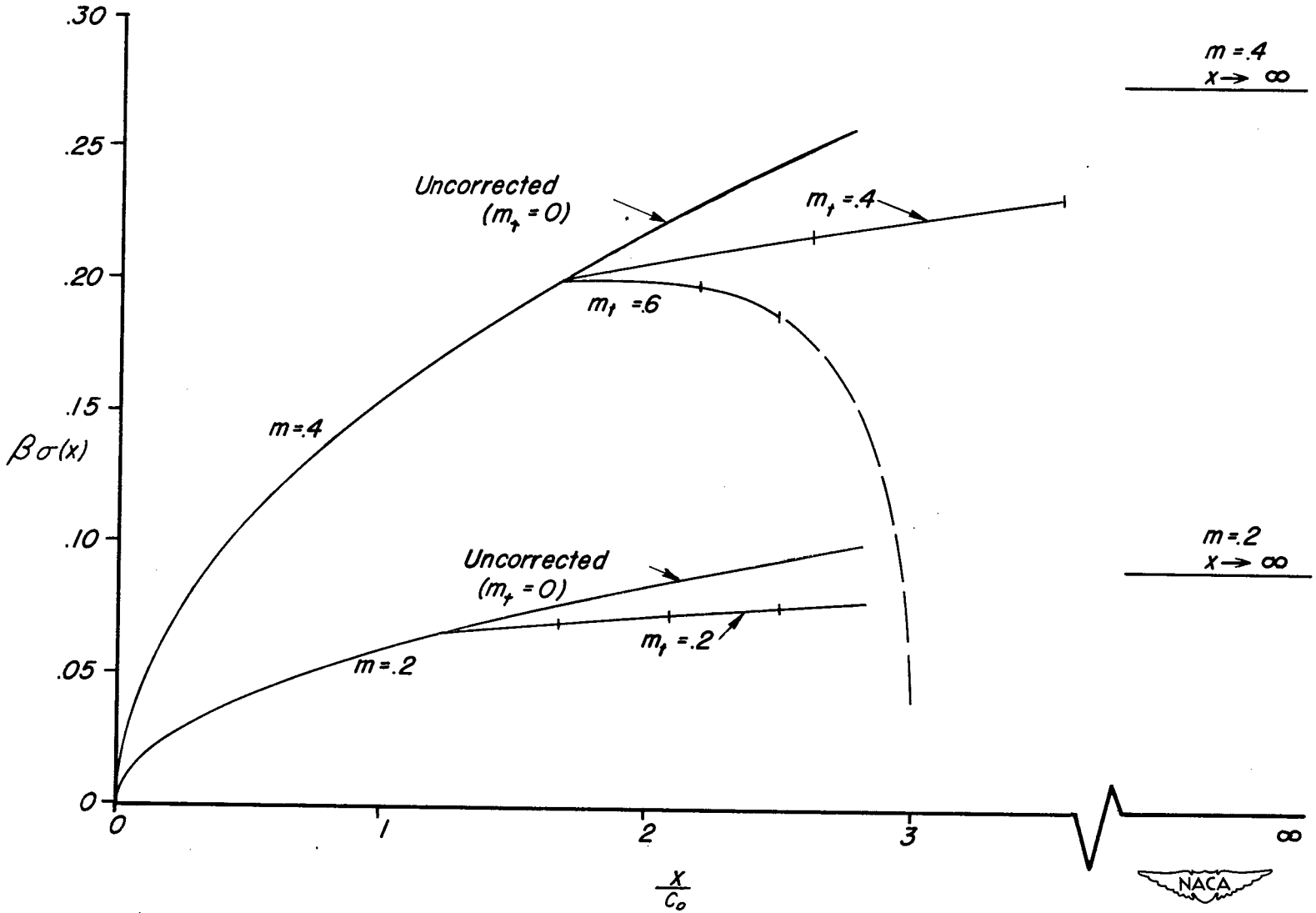

Figure 8. – Leading-edge velocity coefficient σ(x) for correction of two-dimensional load distribution.

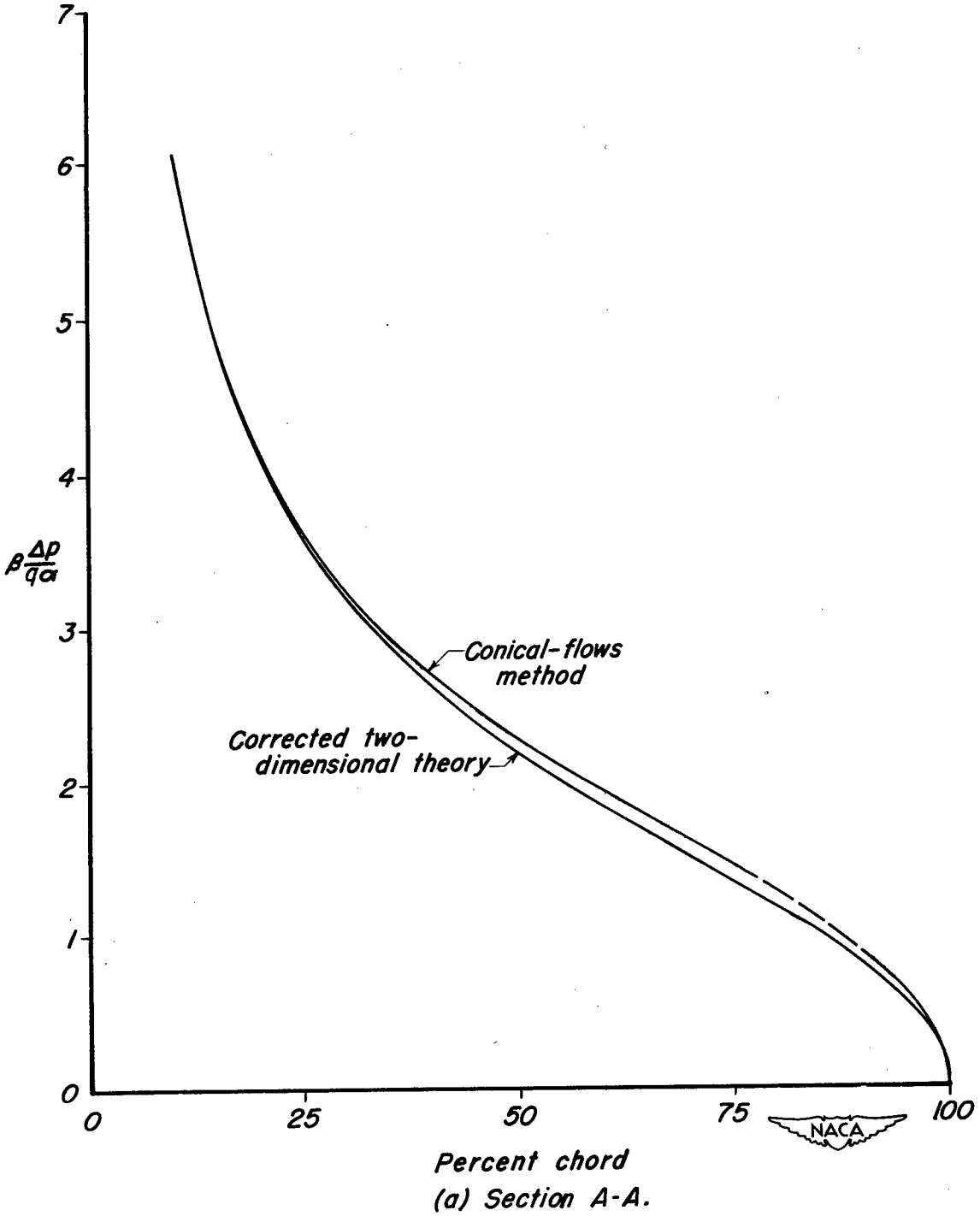

Figure 9.- Load distributions on the tapered wing as calculated by the conical-flows method, and the two-dimensional approximation.

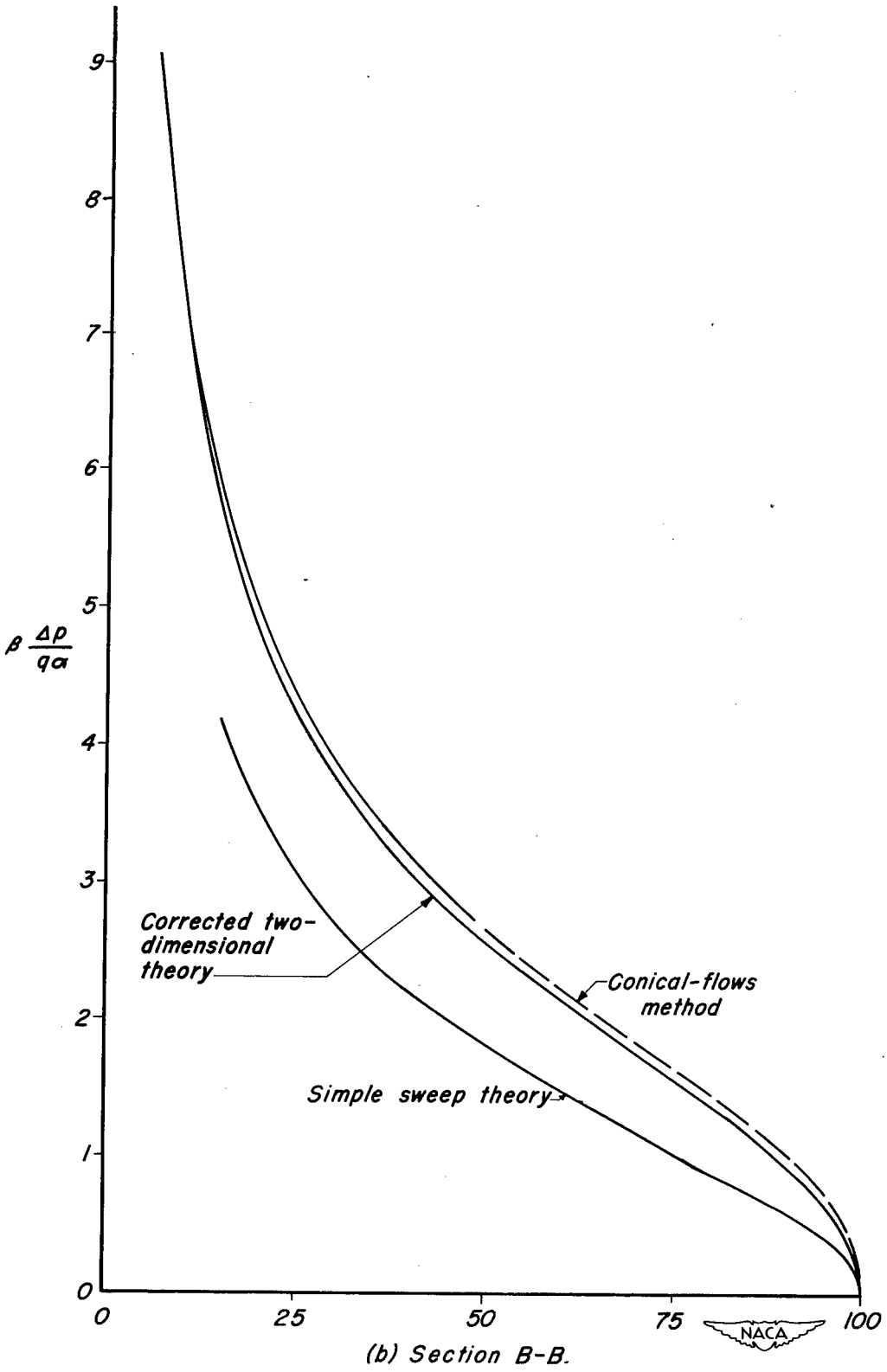

(b) Section B-B.

Figure 9.- Concluded.

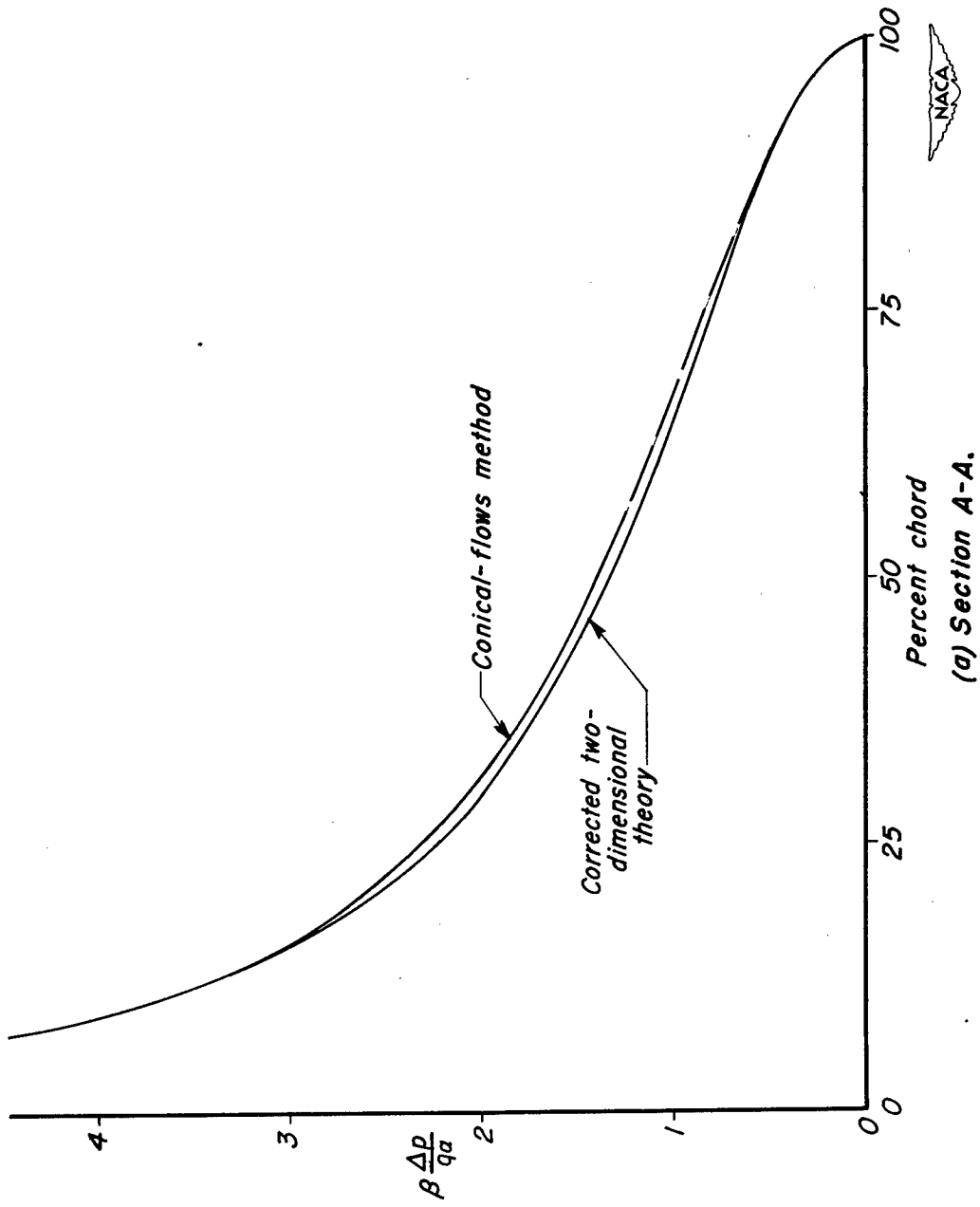

Figure 10.- Load distributions on the untapered wing, m = 0.4, as calculated by the conical-flows method, and the two-dimensional approximation.

(a) Section A-A.

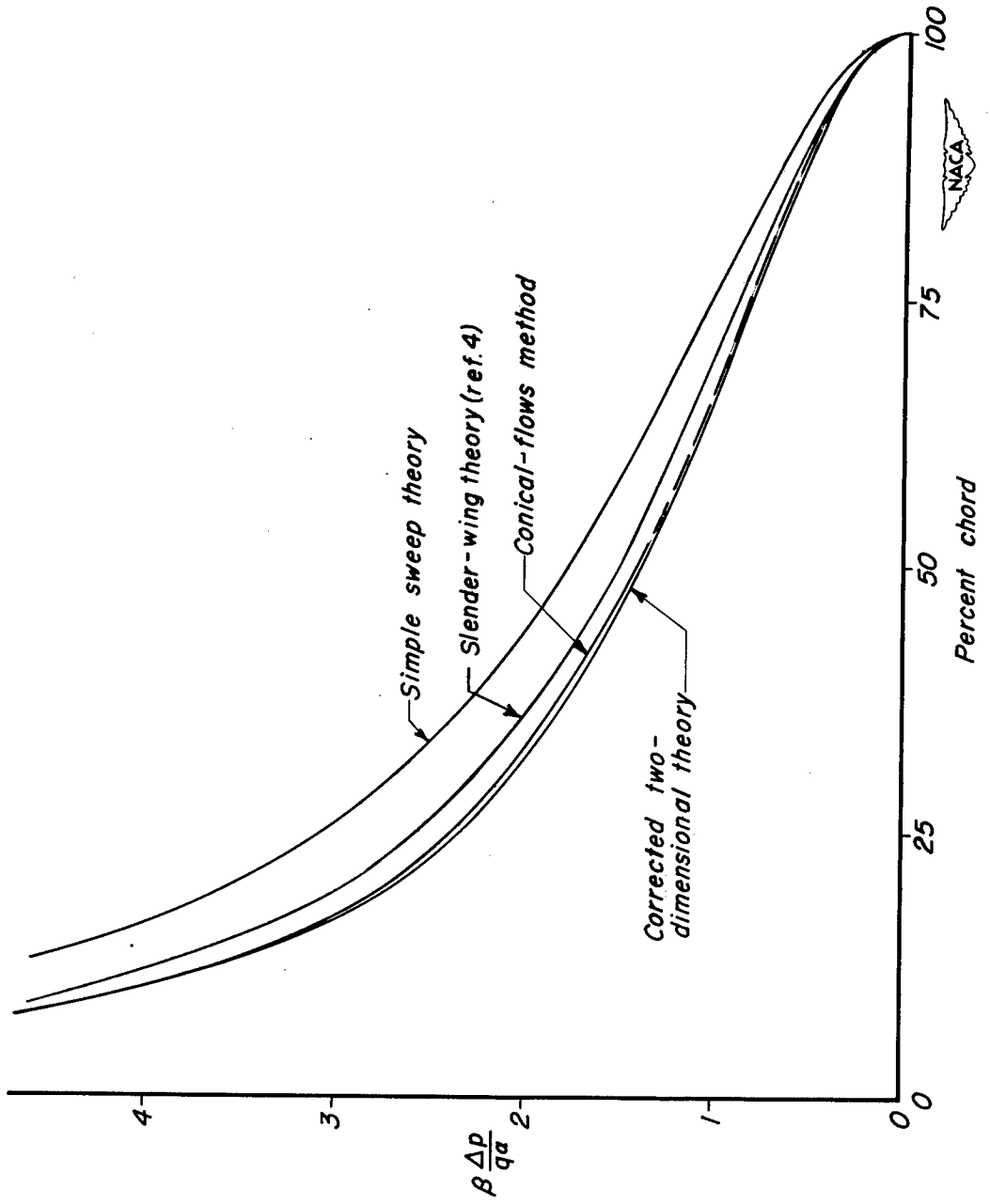

Figure 10.- Concluded.

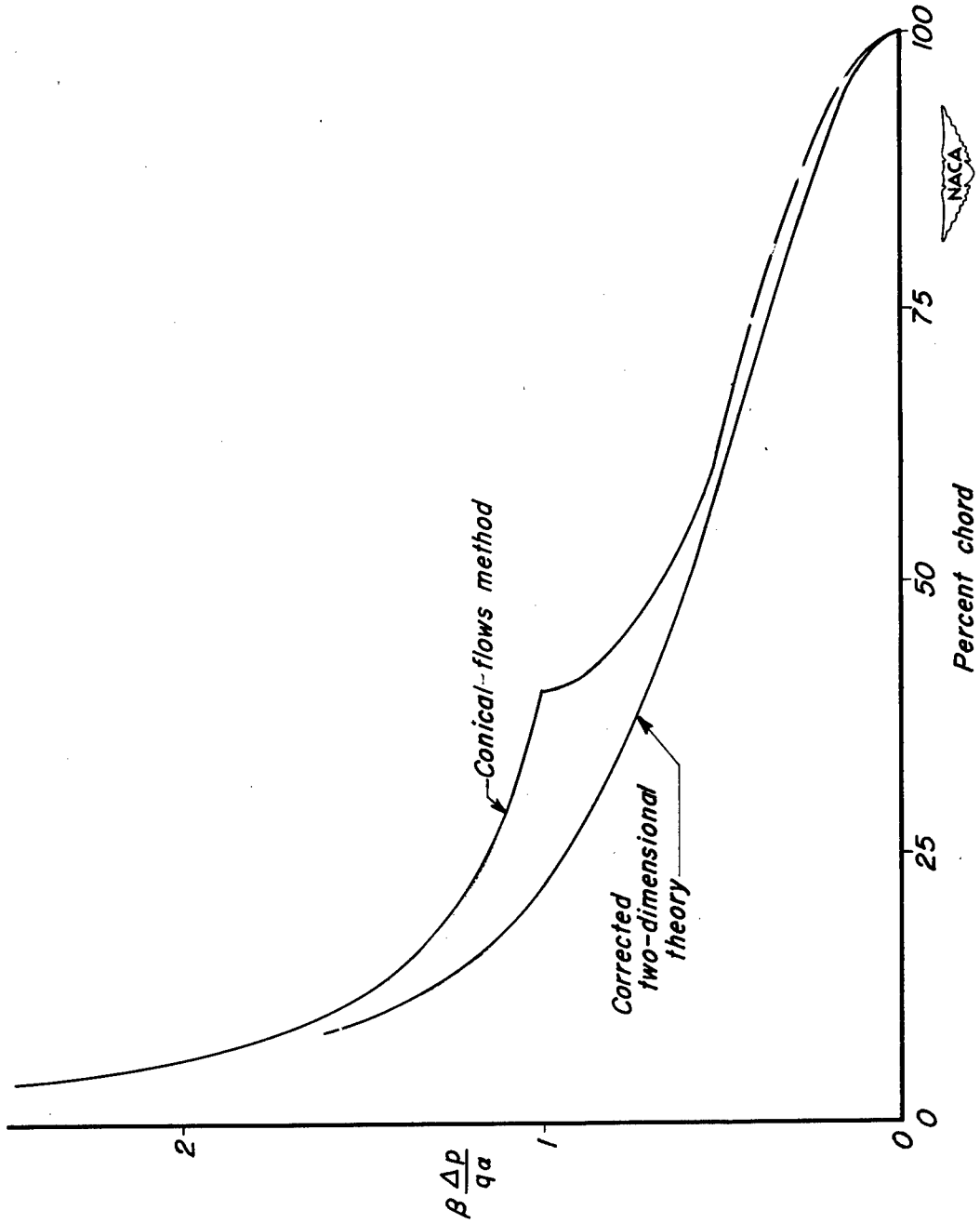

(a) Section A-A.

Figure 11. - Load distributions on the untapered wing, m = 0.2, as calculated by the conical-flows method and the two-dimensional approximation.

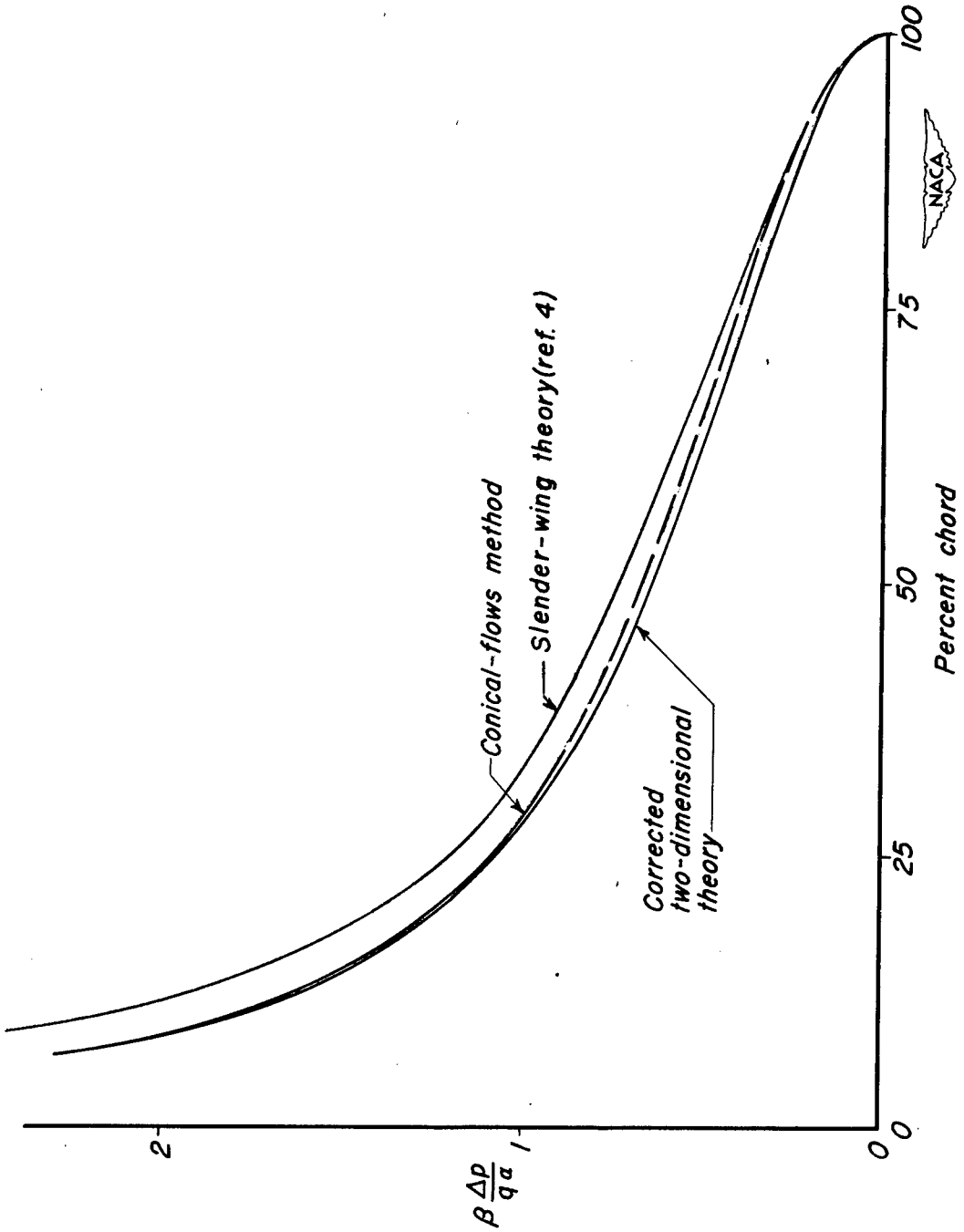

Figure 11.- Continued.

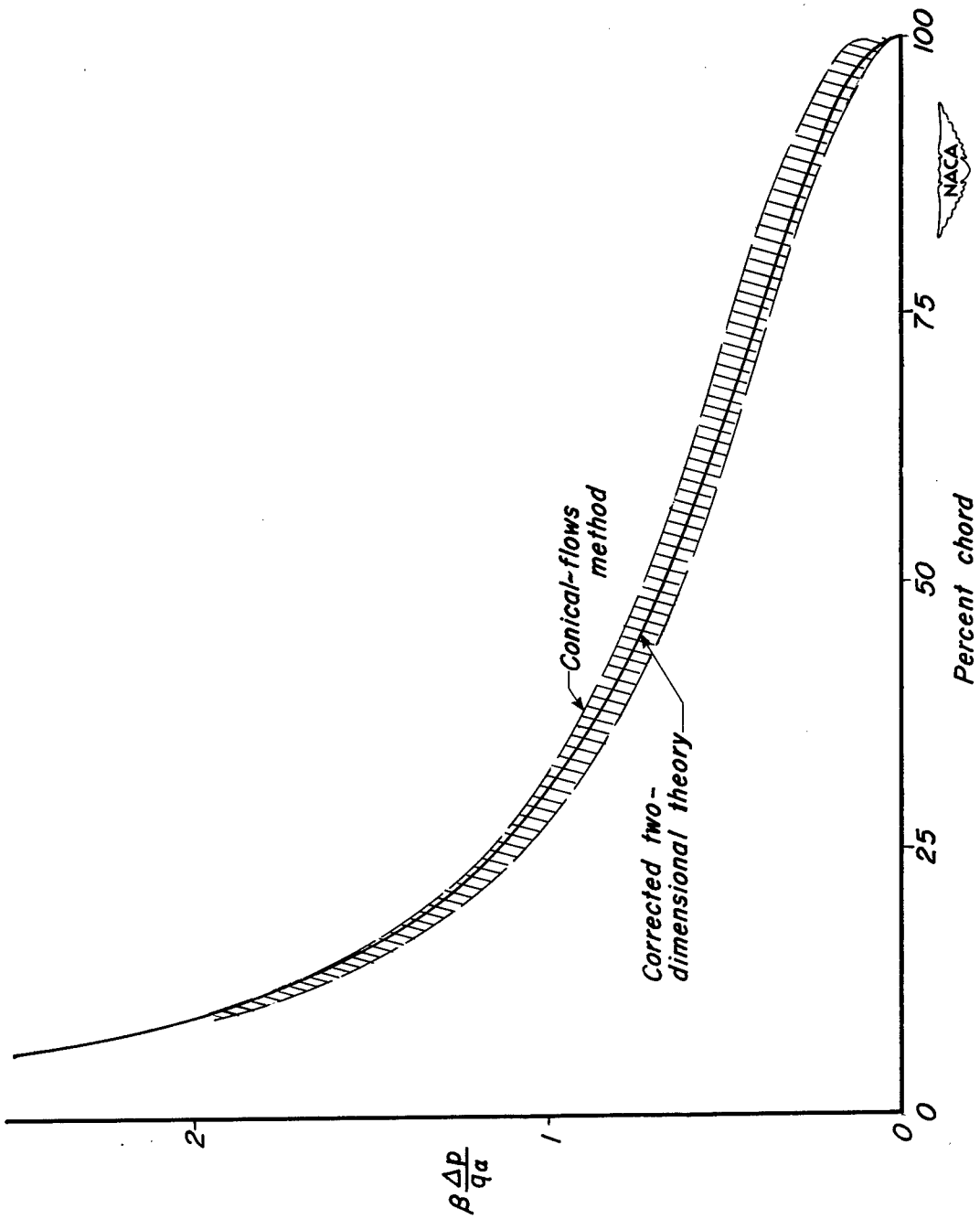

Figure 11.- Continued.

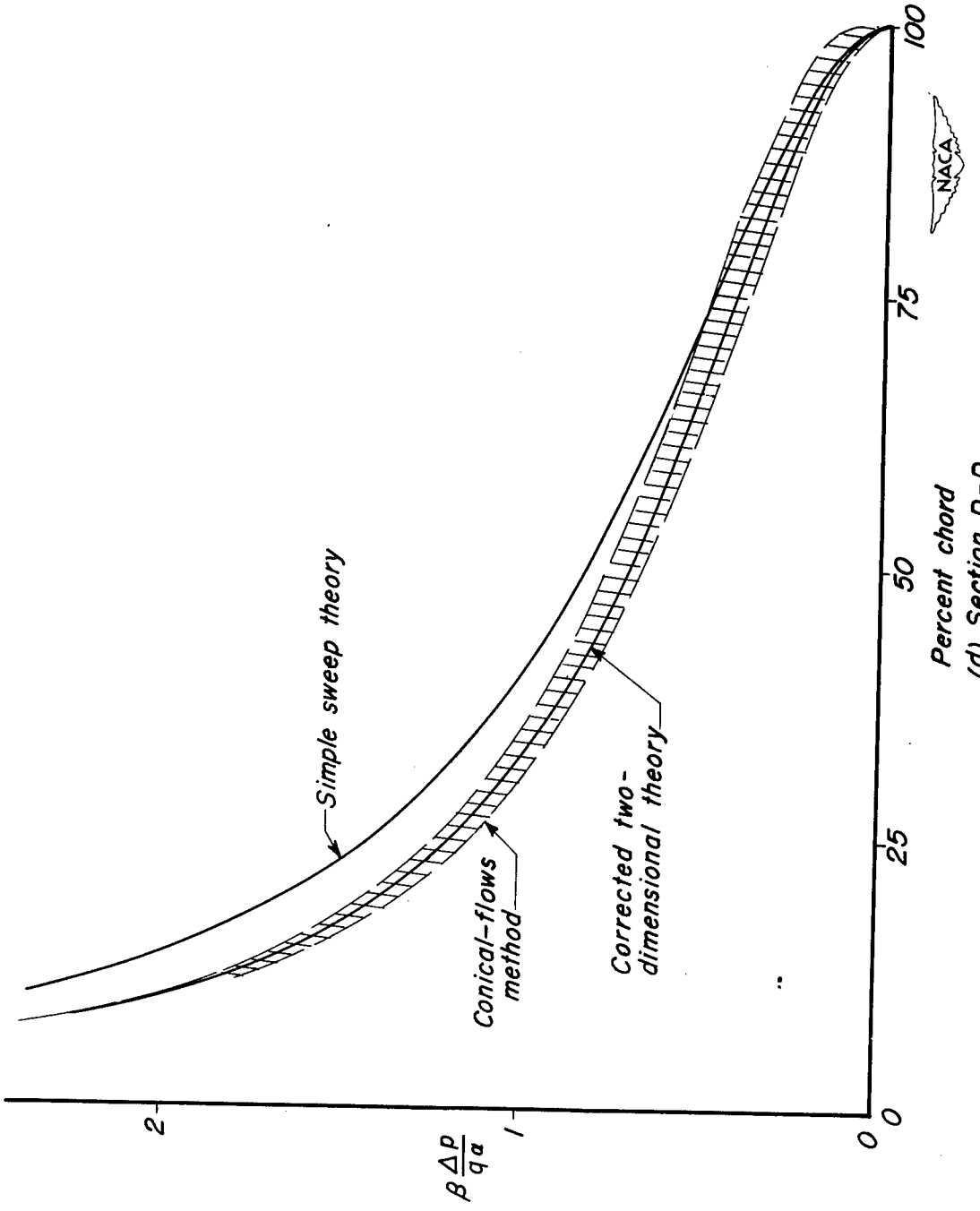

Figure 11.- Concluded.

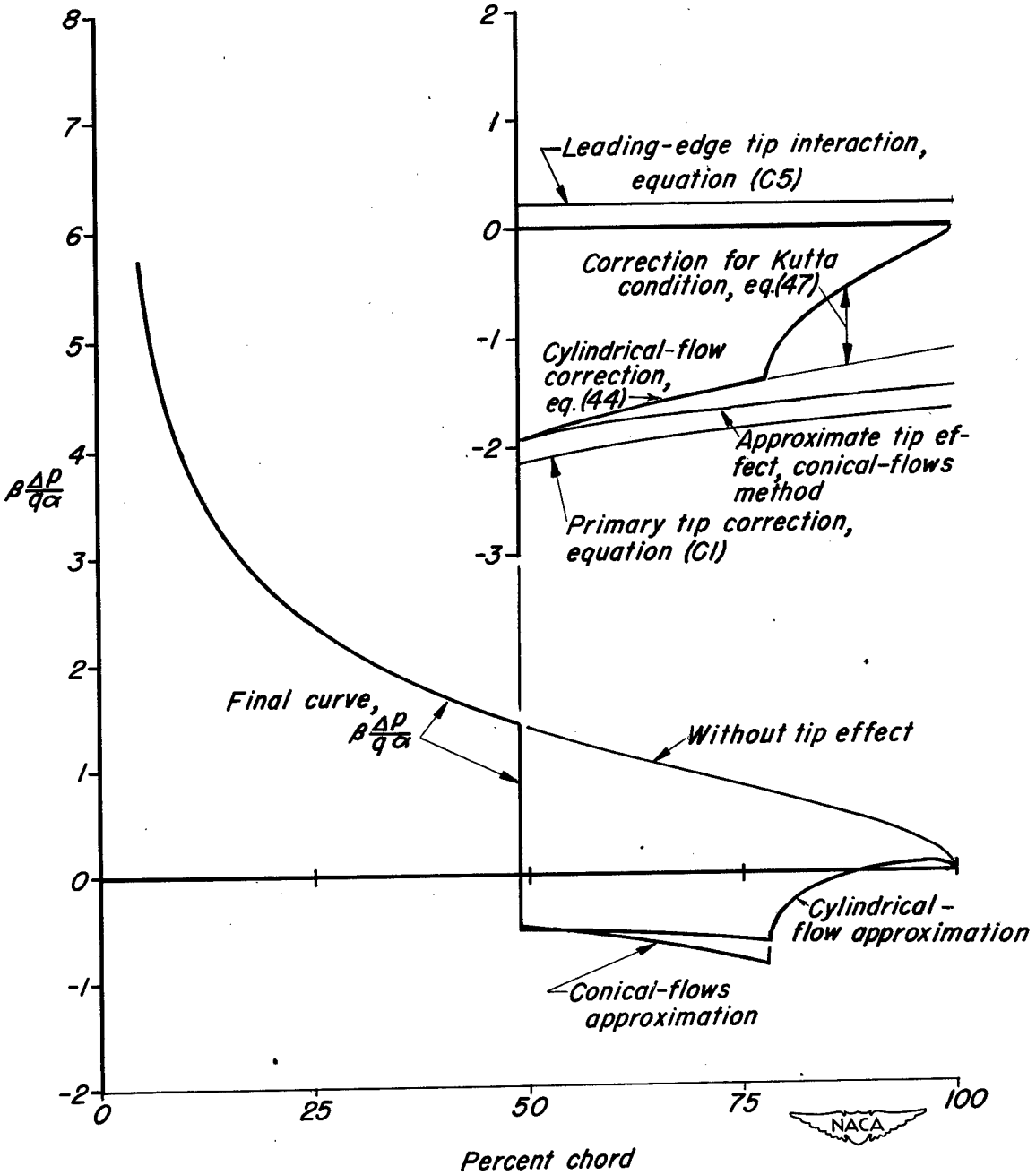

(a) Untapered wing, $m = 0.4$, $\beta A = 1.88$. Section at $\beta y = 0.8c_o$, or 85-percent semispan.

Figure 12.– Load distribution over section near tip as calculated by conical-flows method and by assuming cylindrical flow near tip.

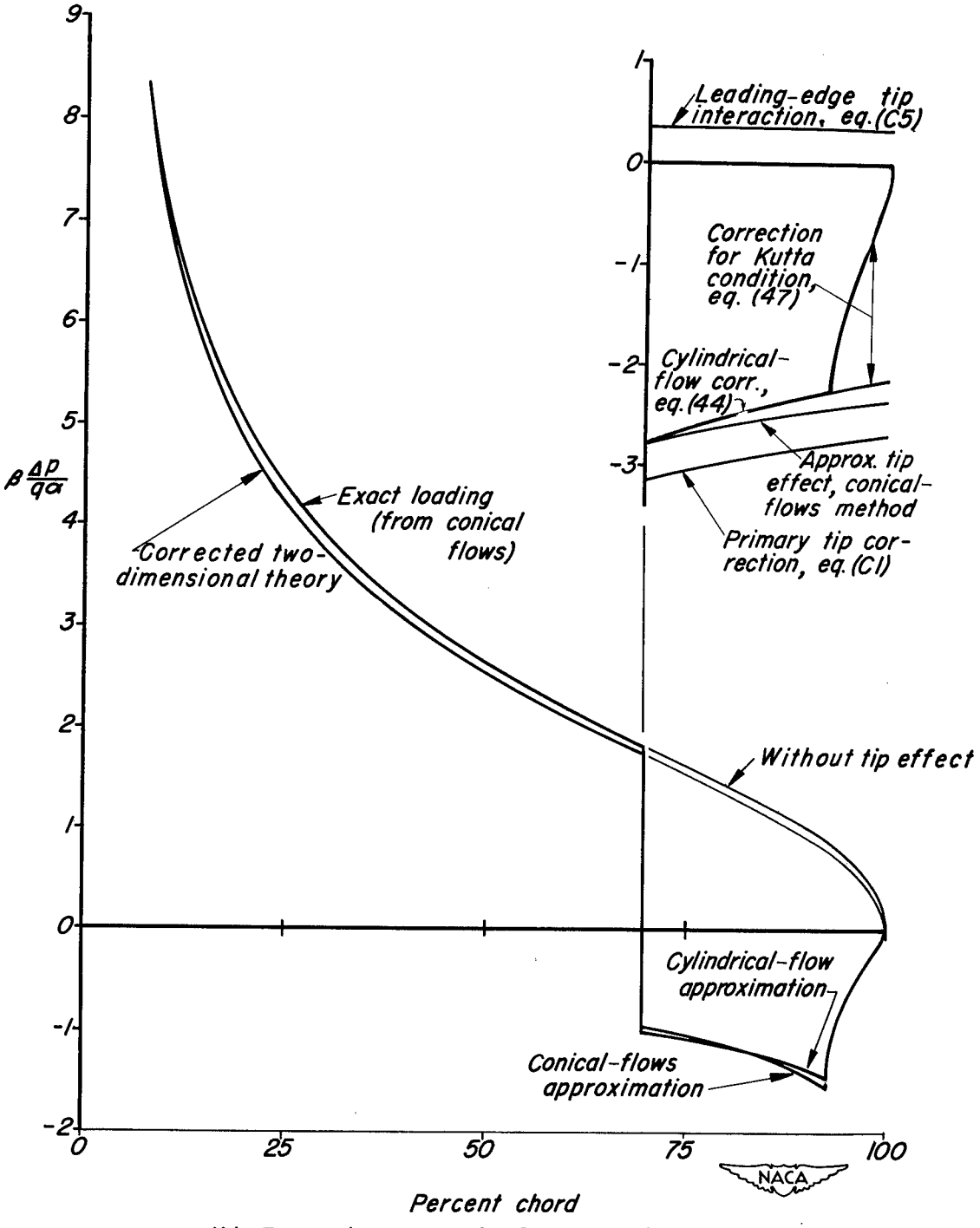

(b) Tapered wing, $\beta A = 2.61$. Section at $\beta y = 0.8c_o$ or 94-percent semispan.

Figure 12.- Concluded.